Stony Brook University

Design of a Robotic Needle Gripper for CT-guided Robotic Needle Biopsy for Lung Nodules

A Thesis Presented

by

Lukasz Krzeminski

to

The Graduate School

in Partial Fulfillment of the

Requirements

for the Degree of

Master of Science

in

Mechanical Engineering

Stony Brook University

May 2011

Stony Brook University

The Graduate School

Lukasz Krzeminski

We, the thesis committee for the above candidate for the

Master of Science degree, hereby recommend

acceptance of this thesis.

Dr. Yu Zhou – Thesis Advisor

Assistant Professor, Department of Mechanical Engineering

Dr. Chad Korach – Chairperson of Defense

Assistant Professor, Department of Mechanical Engineering

Dr. Anurag Purwar – Member

Research Assistant Professor, Department of Mechanical Engineering

Dr. William H. Moore – Outside Member

Medical Doctor, Department of Radiology SBU Medical Center

This thesis is accepted by the Graduate School

Lawrence Martin

Dean of the Graduate School

Abstract of the Thesis

Design of a Robotic Needle Gripper for CT-guided Robotic Needle Biopsy for Lung Nodules

by

Lukasz Krzeminski

Master of Science

in

Mechanical Engineering

Stony Brook University

2011

CT-guided needle biopsy is an important minimally invasive procedure to obtain tissue cells from lung nodules for cytological lung cancer diagnosis. The current procedure requires a specially-trained interventional radiologist to manually advance the needle to the target nodule. Accurate sampling depends on the dexterity and consistency of the clinician and the compliance of the patient. Biopsies in patients who have difficulty in holding breath, small nodules or nodules in the lower-third chest are difficult. Long-time remaining still and holding breath degenerate the patient comfort and compliance. Inaccurate needle positioning and insufficient patient compliance may increase the number of needle passes and occurrence of complications. To addresses these problems, we propose a robotic needle biopsy technique which uses a robot manipulator to place the biopsy needle on a target lung nodule according to the patient's respiratory motion pattern, under the guidance of CT imaging. Comparing with manual technique, the robotic needle placement will bring higher operational steadiness, improve accuracy, and reduce procedure duration. With the ultimate goal to create a clinically applicable CT-guided robotic needle biopsy procedure for lung nodules, the goal of this thesis work is to design the robotic needle gripper, a critical component of the robotic needle biopsy system. This work mainly focuses on the mechanical design and analysis of the robotic needle gripper mechanism. Moreover, for patient safety, the design incorporates a set of force sensors to monitor the forces acting on the gripper, which will trigger the release of the needle under serious force imbalance to protect the patient from serious injury, in particularly under sudden cough or large body movement. Our tests on the robotic needle biopsy prototype show that the proposed robotic needle biopsy can achieve high needle placement accuracy on moving nodules.

Dedicated to

My

Parents

&

My

Grandmother

Table of Content

Table of Figures

List of Tables

Acknowledgments

I would like to dedicate this thesis to my parents and my grandmother who always encouraged me through the most difficult of times. It is due to their financial sacrifice and hard work I was able to receive this college education. I can never thank them enough.

I would also like to thank my advisor Dr. Yu Zhou for his advice and motivational support in this research project. Thanks to Dr. Yu Zhou who encouraged creativity and provided any means of valuable resources this projected excelled beyond a single engineering discipline. The research experience I have gained working with Dr. Yu Zhou is priceless.

I would like also to acknowledge many great faculty members in the engineering department at Stony Brook University who created demanding and challenging learning environment. Thanks to their professionalism and broad educational backgrounds I had opportunity to learn from the brightest people in Stony Brook University. There is no single faculty member I can name without naming all of them. Thank you.

I wanted to thank Dr. William H. Moore from Stony Brook Radiology Medical Center for CT prototype scanning privileges and for the professional overview on this research. Thanks to Dr. Moore who is an expert in performing needle lung biopsies this research gained valuable knowledge in designing this new robotic biopsy system. Thank you.

I would also like to give special thanks to George Luhrs and Lester Orlick, the two machinists who helped in developing the prototype which is a solid foundation for this research. I very grateful for their professional advice and unlimited aid I have received during my countless hours in the machine shop.

I wanted to thank the author Terese Winslow for granting permission in using two copyright images illustrated in Figure 1.1 and Figure 1.2. Thank you.

I would finally like to give thanks to all my colleagues who aided me in this research and many other projects. I would to give special thanks to Xiaoyu Chen for early design work on this project and Kaarvannan Thiruvalluvan for assistance in testing the prototype. I have learned that team work is the most important part of engineering.

CHAPTER 1 – Introduction

1.1 Lung Biopsies Background

Today lung biopsies are performed to verify abnormalities called nodules which are visually detected using x-rays and high resolution CT scanners [1]. The biopsies samples are collected for examination purposes to diagnose variety of diseases such as cancer, tuberculosis, pneumocystis, sarcoidosis, pulmonary fibrosis, or other causes such as drug reactions. The biopsies can be collected uses different techniques which application depends on nodules location and patient's health [2]. The preferred biopsy techniques are non-surgical procedures which are less invasive and require shorter recoveries for the patient's. The other benefits of non-surgical are lower complications that are more common with more invasive procedures [3]. There are currently two non-surgical techniques in use known as bronchoscopy and needle biopsies.

The bronchoscopy biopsy is performed in cases when abnormalities are located in the air passage or near the air passage in the lungs. The tissue collection begins with a devices called a bronchoscope which uses a lighted tube which travels from the mouth or nose into the lungs as illustrated by the Figure 1.1. The physician controls the traveling lighted tube mechanically under real-time feedback from the small camera located at one end. The bronchoscope has also the ability to remove abnormal growths and collect sample using mechanical jaw which also located at the end of the tube [4].

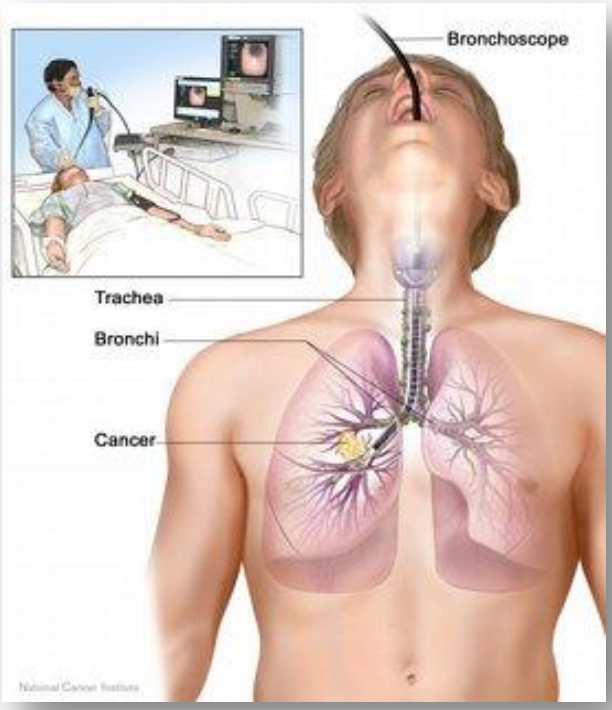

Figure 1.1: Bronchoscope lung biopsy.

The needle biopsy is performed when an abnormal nodule is located away from the air passage and is unreachable by the bronchoscope. In this case a hollow needle with a sharp insert will be placed through the lung into the center of the nodule as illustrated by the Figure 1.2. This procedure will require the patient to be fully awake with only local anesthesia to numb the passage area of the needle. The patient is also required to hold breath during certain parts of this procedure [5]. There will be careful planning performed by the physician to determine the correct point of entry to reach the nodule. The CT scanner will provide image feedback in confirming the needle location. The CT scanner will be used in cycling mode (non-real-time) to reduce radiation exposure on the patient [6]. For each CT cycle mode scanning the clinician will evacuate the exposure room. The needle placement will be carried out in series of steps which require CT scanning to confirm needle location. The needle is designed with measurement grid which the clinician uses to determine the depth of the insertion. This non-real-time feedback system requires experienced clinician in determining the distance and the angle required during this series of steps targeting procedure [7]. In case when the needle is unable to reach the nodule the clinician may attempt another point of entry from another location. When finally the needle reaches the target the sharp insert is removed from the needle and the syringe is attached to draw in the sample. After

sufficient sample is collected the clinician removes the needle and the procedure is completed [8].

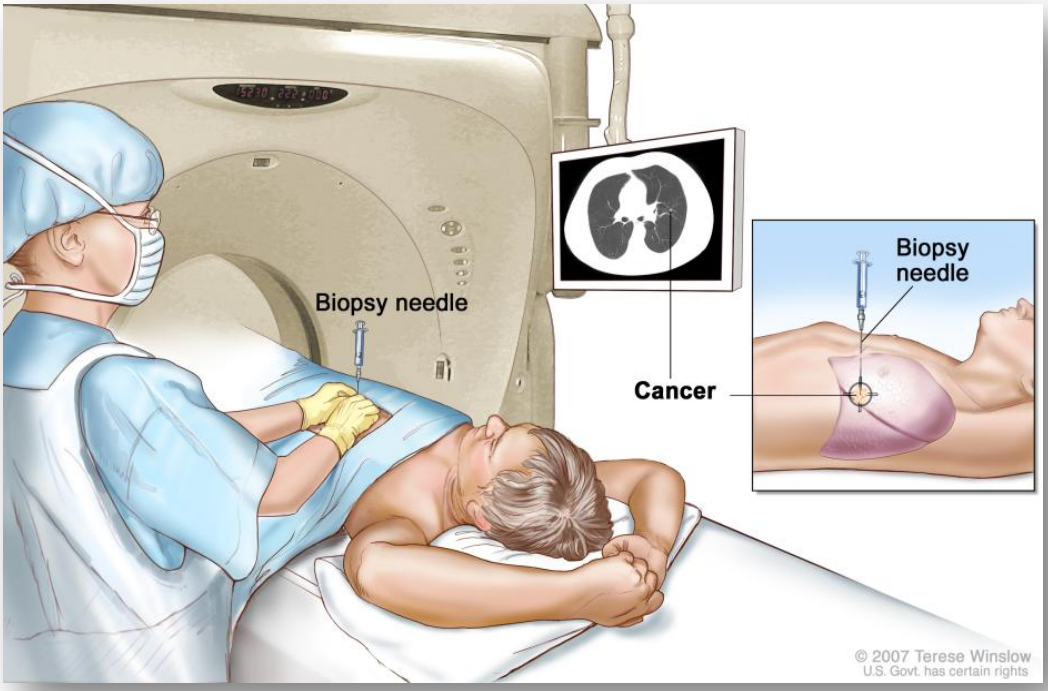

Figure 1.2: Needle lung biopsy.

1.2 Objective and Motivation

The objective of this research is to improve the current needle biopsy procedure. The challenges facing needle biopsies are noted in manual targeting and radiation exposure from CT scanners. The current procedure requires a specially-trained interventional radiologist to manually advance the needle to the targeted nodule. Accurate sampling depends on the dexterity and consistency of the clinician and the compliance of the patient. Biopsies in patients who have difficulty in holding breath, small nodules or nodules in the lower-third chest are difficult [9]. Long-time remaining still and holding breath degenerate the patient comfort and compliance. The risks associated with manual lung biopsy increase when the

needle requires additional attempts to reach the target [10]. Multiple needle insertion can result in complication where the lung will not seal in time causing a condition known as Pneumothorax (lung collapse) [11]. There are present limitations on targeting capability due limited accuracy using manual needle placements with non-real-time feedback as a correcting factor. With complications in difficult targets the CT scanner use will increase resulting in higher radiation levels [12]. There are other surgical biopsies options available when minimum invasive methods are unable to collect sufficient samples. However, the known problems associated with these more invasive techniques are longer recovery time and higher complications risks. In some cases the complications risks using surgical biopsies can outweigh the benefits of nodule diagnosis [13].

1.3 Proposed Solution

The solution that we want to propose is a new robotic needle biopsy system which uses a robotic manipulator for placing the needle on target (Figure 1.3). The proposed robotic needle placement system consists of a robotic manipulator and a robotic needle gripper (end-effector) with remote controls. When compared with manual needle biopsy technique, the robotic needle placement will bring higher operational steadiness, improve accuracy, and reduce procedure duration. The robotic needle placement enhances the positioning accuracy and operational steadiness, avoids human inconsistency and subjectivity, and results in more accurate and efficient needle biopsy. In this biopsy procedure the clinician controls the robotic system from outside the exposure room. This limits radiation and creates a safer working environment for the clinician. This new biopsy technique functions in collaboration with patient's respiratory motion pattern without breathing interruptions. With this new technique now patients who had difficulty holding breath will experience less discomfort. The patient respiratory motion under stable breathing pattern will be modeled for optimal needle placement path using CT scanner under real-time feedback. The fast robotic operation guided by the respiratory motion model will substantially shorten the procedure duration, which helps to improve patient comfort and reduce radiation exposure. For safety, a sensory force feedback system with automated self-needle release had been adopted into the robotic needle gripper. The sensors will provide real-time feedback to monitor for abnormal flexing forces on the needle. Finally, if the proposed research will be successful this new biopsy technique will lead to safer, more reliable, and more precise lung biopsies.

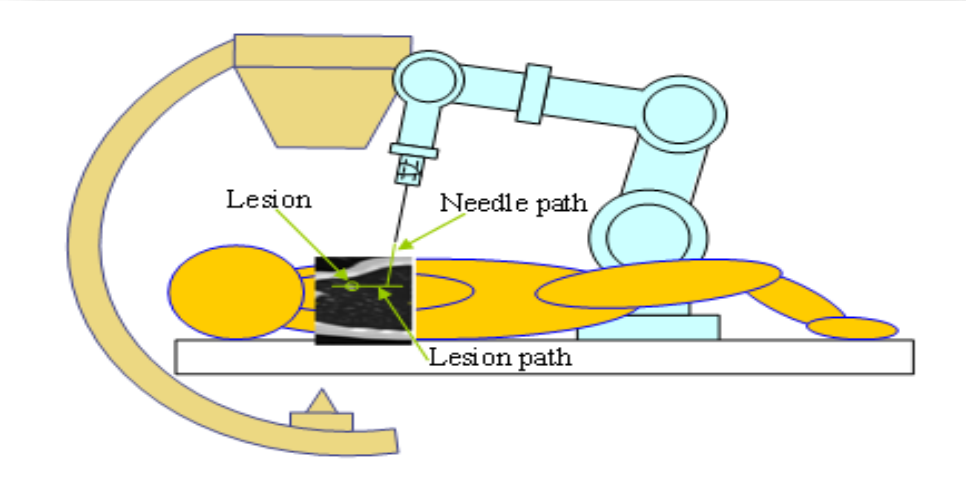

Figure 1.3: The proposed new robotic system for needle lung biopsies.

1.4 Procedure

The design of robotic biopsy system illustrated by Figure 1.4 operates on the similar biopsy principles as used in traditional technique. The correlated difference between two techniques occurs during needle placement. In traditional technique the physician has responsibility for targeting and using hand skills for placing the needle on movable nodules. The difficulty in this task occurs when during breathing the lungs outer layers and the nodules inside the lung can move in opposite directions [14]. Now to improve this task the robotic manipulator will replace physician role in manually placing the needle on target. The six degree of freedom robotic manipulator will function as the needle placing force behind this biopsy procedure. The special designed needle gripper attached to the robotic manipulator as the end-effector will retain the needle until the release has been engaged. The force sensors incorporated into the needle gripper design will provide feedback during needle placement. For safety, automated system has been added to release the needle during sudden unpredictable motion. The final biopsy collection will be carried out the same way as in tradition techniques using a syringe. In this case, after the needle will be placed on target, the needle gripper will release the needle and the physician will carry out the final biopsy procedure.

Figure 1.4: The proposed prototype of end-effector for robotic biopsy system.

CHAPTER 2 – Needle Gripper (End-Effector) Design

2.1 Introduction

The needle gripper prototype has been designed to provide safe, accurate, and efficient needle biopsy procedure with superior results from current practice. The improvement of the current biopsy procedure requires this end-effector design to meet the highest standard in reliability and function. The descriptive design features which will be discussed in this chapter are design overview, design constraints, design material, structure design, mechanism design, electrical control design, function and operation, needle loading procedure, and vibration reducing dampers.

2.2 Design Overview

The end-effector has been designed to accommodate all the function required during the robotic biopsy procedure. In Figure 2.1 the illustration shows a complete needle gripper proposed prototype design. The complete details of this design will be explained in other section of this chapter. The end-effector operational environment which requires a CT scanning feedback during biopsy procedure has constraint the material used in this design. The reason for specific material is CT image interferences that are known to occur with material from metallic origin. However, the main purpose of this design is to constrain biopsy needle during procedure until release is commanded by the control system. For this prototype a combination of mechanical and electrical systems are designed to allow remote needle release. The mechanical design includes a gripper and trigger mechanism for which the source of needle release energy is a compressed helical spring. The needle release function starts by releasing the compressed helical spring energy using the trigger component of the trigger mechanism. The released spring energy activates the gripper mechanism which releases the needle. For electrical control release a solenoid is used to activate the trigger mechanism from remote location. In Figure 2.2 the illustration shows an overview of the trigger and the gripper mechanism controlled by the solenoid.

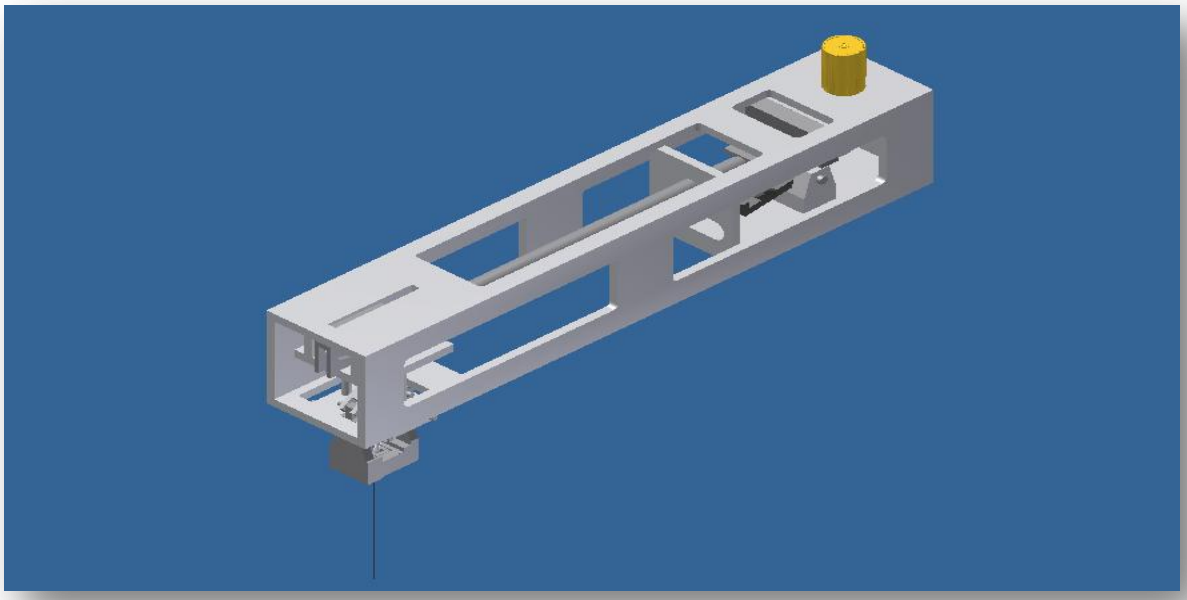

Figure 2.1: Proposed needle gripper (end-effector) prototype.

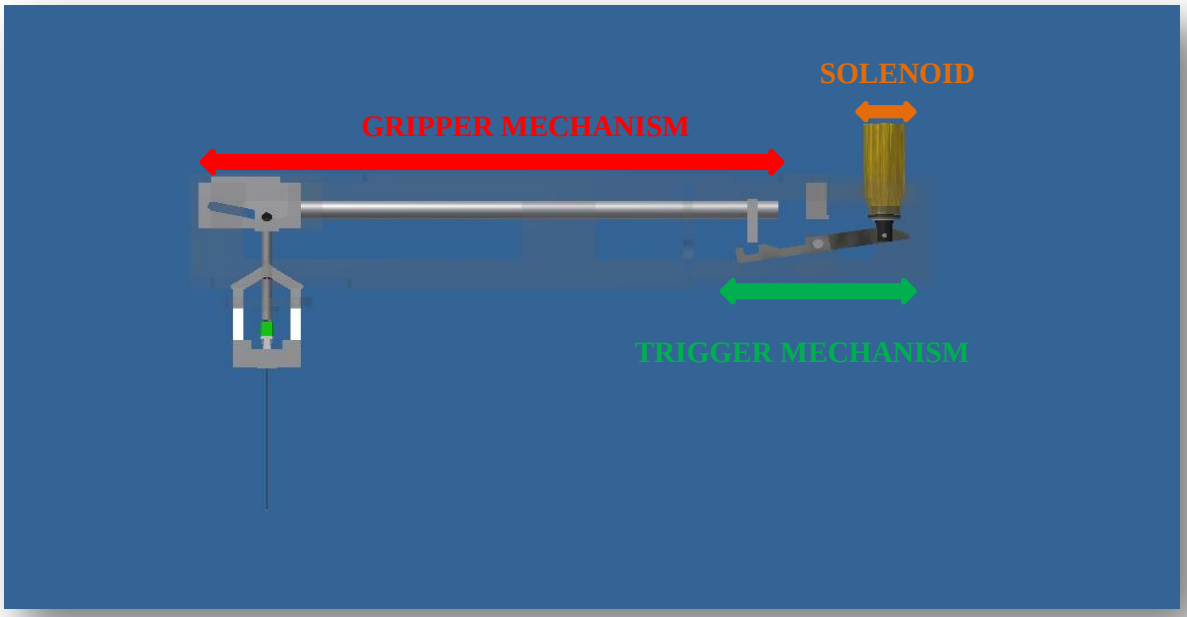

Figure 2.2: The configuration of two mechanisms controlled by a solenoid.

(Helical spring not shown)

2.2 Design Constraints and Solutions

The end-effector is designed with constraints placed on material, strength to weight ratio, and mechanical-electrical controls. The first and most critical constraint of this end-effector prototype is the design material. The end-effector is designed for medical environment which requires close vicinity CT scanning of the prototype. The solution has been proposed to design the end-effector without metallic components which can affect the image quality of the CT. For these reasons a specific material called Acetal Copolymer has been the choice for this design. This material has good structural and mechanical properties which have been used as the primary design material for this prototype. The second constraint that has been placed on this design is the strength to weight ration. The end-effector has been constraint to a maximum weight of 2.3 kg (5 lbs.) due to lifting capacity of the robotic manipulator. The solution was to design a light weight structure which will concentrate the structural rigidity toward the insertion force on the needle. The third constraint was placed on mechanical-electronic controls design. The purpose of this system is to provide means of mechanical needle release using electronic controls. For this the mechanical design has been introduced to release the needle using an electrical device called a solenoid. With the use of helical spring the control system is able to achieve almost an instantaneous needle release.

2.3 Design Material (Acetal Copolymer)

This prototype has been developed from FDA compliant, engineering thermoplastic, called Acetal Copolymer (Figure 2.3). The properties of this material made it applicable in structural, mechanical, and clinical applications. In structural application, the stiffness, high tensile strength, and fatigue endurance properties had given this design sufficient strength to weight ratio. In mechanical parts design, the contribution of low coefficient of friction and high wear resistance property provides extended services life without recommended service intervals. In clinical environment the advantages of using this material are stability in moisture and resistance to most chemicals at elevated temperatures. In addition, this thermoplastic can be sterilized using EtO gas or steam autoclaving without a loss of mechanical or structural properties. The disadvantage of this material had been noted in

bonding difficulties and structure weakening under specific type of chemicals. The problem of Acetal prevents most glue from providing sufficient bonding strength. Special surface treatment can improve bonding but with limited results when comparing to other plastics. In case of chemical degeneration, Acetal has poor resistance to chlorinated water and acids. When the surface is exposed to these specific chemicals the corrosive stress can develop into cracks leading to structural failure. In prevention to this chemical degeneration the structure has been design with a safety factor multiple times the operational force.

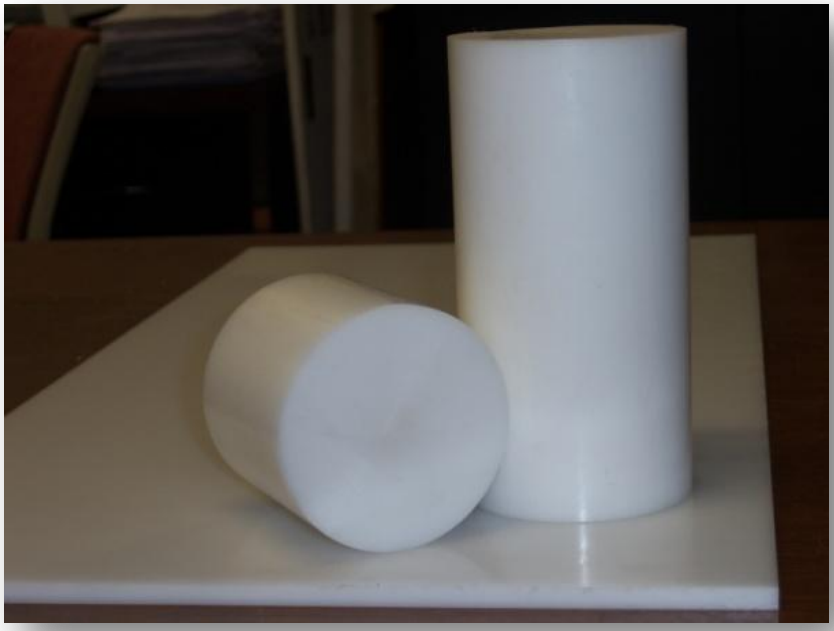

Figure 2.3: Acetal Copolymer used in manufacturing of the prototype.

2.4 Needle Gripper Design Dimension

The dimensions in this end-effector have been determined in relation to structure rigidity, mechanism space requirements, and critical metallic components location. The metallic components such as the helical spring and the solenoid are separated from non-metallic components by a safety distance of 25.4 cm (10 in) from the needle location. This

requirement will be justified in Chapter 6 during CT scanning testing. The end-effector design dimensions are illustrated in Figure 2.4

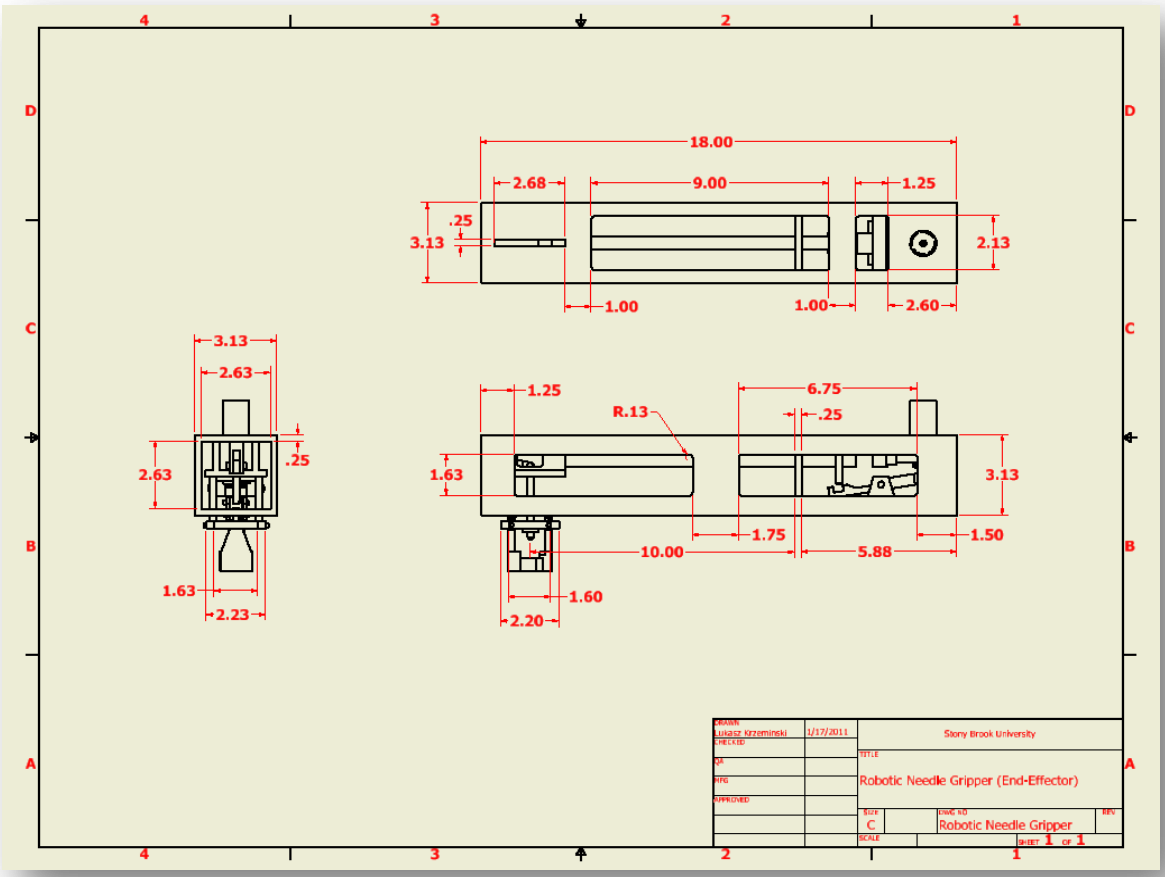

Figure 2.4: The prototype design dimensions (inches).

2.5 Structure Design

The structure for this prototype has been designed to be lightweight, structurally stable, non-metallic, and simple to manufacture. With these constrains applied the optimum design had become a rectangular shape structure fabricated from stock sheet of Acetal

Copolymer. The rectangular design provides excellent stability in deflection while providing sufficient housing for other components. The simplicity of this design reduces manufacture time due to symmetry and interchangeability between components during initial fabrication. The fabricated rectangular sides are assembled using non-metallic screws from nylon. The chemical bonding using glue would be more efficient however the property of this material limits this application. For reduction of weigh this rectangular prototype had been designed with special cutouts on its sides without significant compromise on vertical deflections as illustrated by the Figure 2.5. The stress analysis performed in Chapter 3 will reveal stability of the prototype structure.

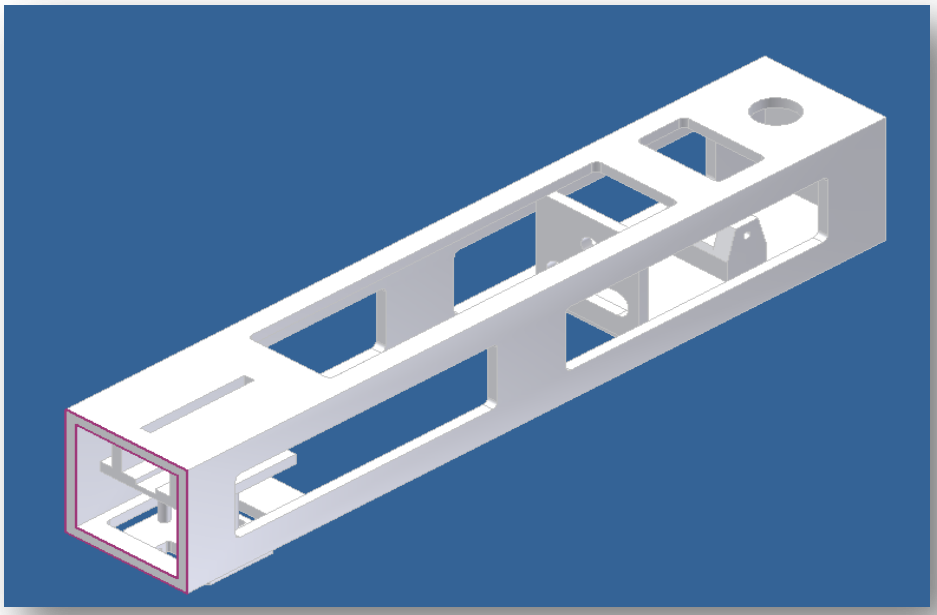

Figure 2.5: Structure design of the prototype without components.

2.6 Mechanism Design

The needle gripper is design with a specific mechanical function to secure and release biopsy needle using electronic controls. This mechanical design is a combination of dual mechanisms referring to them as the trigger and the gripper. The combination function of

these dual mechanisms classifies this system as 1 DOF when system is loaded and 2 DOF when system is unloaded. The needle release mechanical function including electronics will be disclosed in detail in Section 2.8. The parts summary below (Figure 2.6) will define the basic function and purpose for each major component from each mechanism.

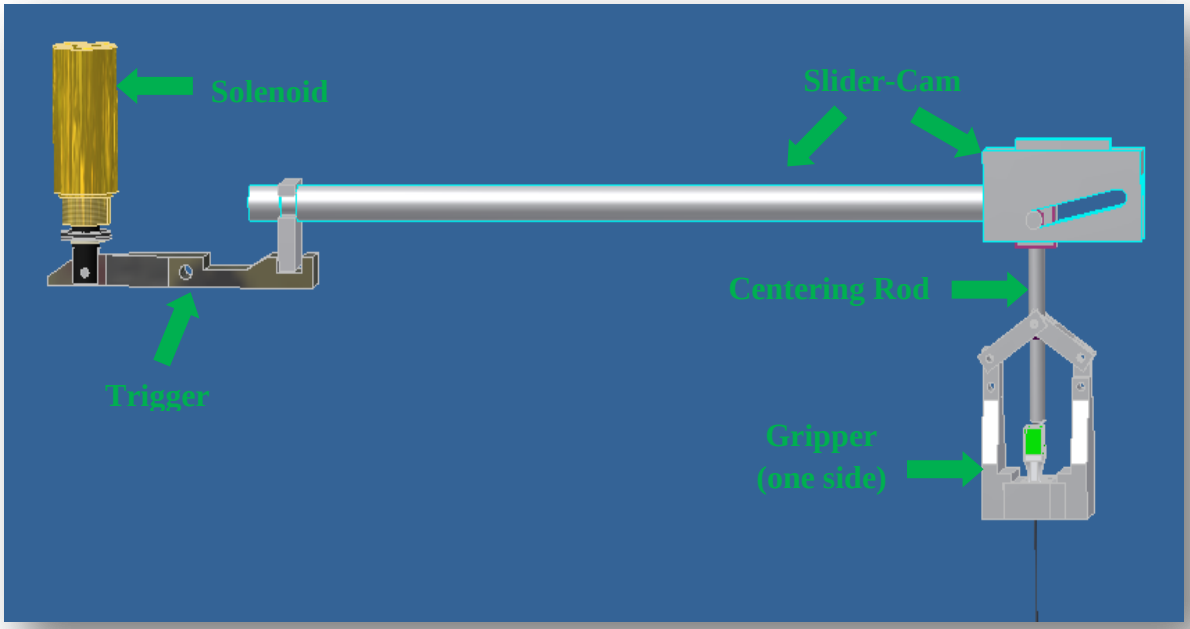

Figure 2.6: Mechanical schematic of all major components and the activation solenoid.

(Helical spring not shown)

Gripper Mechanism

- Grippers

The purpose of the gripper is to provide secure-hold and non-straining needle release during biopsy procedure. The two side grips are the main components that provide horizontal stability for the needle.

- Centering Rod

The centering rod carries the vertical force from the needle while keeping the needle always aligned. The centering rod is also synchronized with the gripper motion in locking and releasing the needle according to slider-cam position.

- Slider-Cam

The slider-cam component transfers motion from horizontal into vertical. In this setup the slider-cam is a horizontal input energized by the helical spring and the output is the vertical centering rod constrained to the grippers. The importance of the slider-cam design is responsible for sufficient mechanical advantage in providing a firm lock on the needle.

- Helical Spring

The helical spring is the energy source of the gripper mechanism. The stored potential energy in the spring provides almost instantaneous gripper release by pulling the slider-cam horizontally.

Trigger Mechanism

- Trigger

The trigger component provides temporary holding support for compressed helical spring and attachment to metallic rod of the solenoid. The magnetic pull from the solenoid results in the trigger to rotate and release the energy of the helical spring.

2.7 Electrical Control Release

The electrical control release system of the prototype consists of electromagnetic component called a solenoid and remote controller. The full electrical control detail design will be explained in Chapter 5. The summary below will define the basic function and purpose for better understanding of the system. The electromagnetic solenoid function with mechanical components is illustrated in Figure 2.7.

Electrical Control

- Solenoid

  The solenoid is electromagnet which uses electricity to generate a magnetic field. In this case the solenoid generates a pulling force on a metallic rod which has been attached to the trigger mechanism. In result, the trigger mechanism releases the compressed helical spring which energizes the gripper mechanism.

- Remote Controller

  The remote controller controls voltage transmitted to the solenoid which is required to generate magnetic field.

2.8 Function and Operation

In this section the mechanical function of the prototype will be discussed in detail. The illustration in Figure 2.7 will show a sequence of events that take place almost instantly when needle is released. The individual component function will be summarized according with the numbered events from the Figure 2.7. The sequences of events are as follows:

1) The magnetic field of energized solenoid provides a pulling force on the trigger at point {1}.
2) The trigger experiences rotation taking place around constrained pin at point {2}.
3) The trigger releases the slider-cam from the locked position and helical spring is discharged at point {3}.
4) The slider-cam begins to accelerate as the helical spring continues to discharge at point {4}.
5) The slider-cam continues to accelerate at point {5}.
6) The pin attached to the centering rod begins to slide vertically in relation to the slider-cam at point {6}.
7) The centering rod begins vertical motion at point {7}.
8) The gripper arms attached to the centering rod and the grippers using pins begin to move at point {8}.
9) The grippers begin to experience rotation around constrained set of pins at point {9}.
10) The centering rod moves always from the top portion of the needle at point {10}.

11) The grippers move away from both horizontal sides from the needle resulting in release at point {11}.

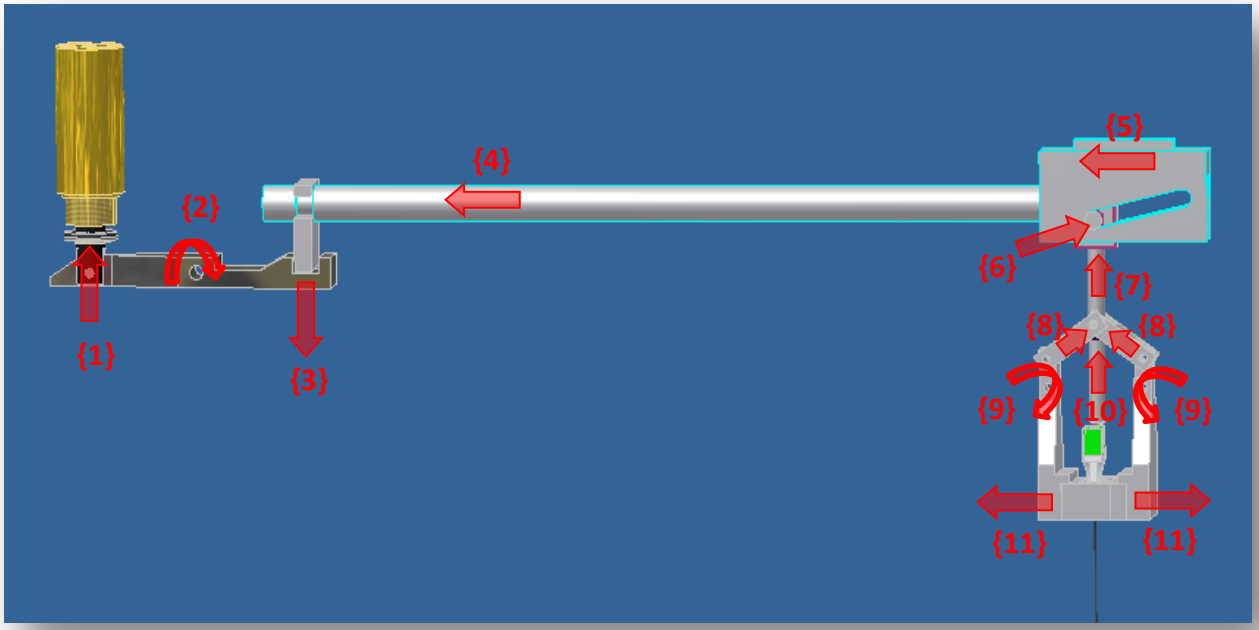

Figure 2.7: Description of component mechanical function for releasing the needle.

(Helical spring not shown)

2.9 Needle Loading Procedure

In preparation for biopsy procedure the needle requires to be secured in the needle gripper. The procedure to reload requires placement of the needle against one side of the gripper while horizontally pulling on a loading lever toward the grippers (Figure 2.8). As the lever will begin to move the helical spring will compress and the two grippers will begin to close around the needle. The loading level will require to be pulled until the trigger lock will engage. After the lock is engaged the needle and the handle can be released and the system is ready for biopsy procedure. The end-effector design requires manual reloading every time the needle is released.

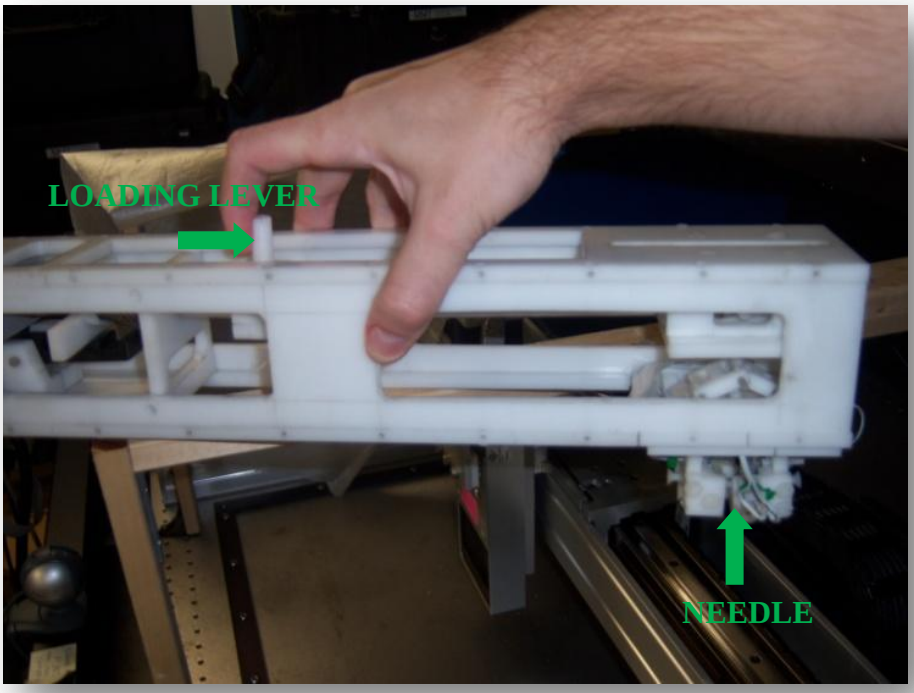

Figure 2.8: Needle loading procedure into the needle gripper prototype (end-effector). (Needle not shown)

2.10 Vibration Reducing Damper

The mechanism developed for the prototype depends on helical spring to energize the release of the needle. In result the excess energy from the spring transfers to vibration which can transmit to other critical components. In early gripper testing a failure of the stepper motor had occurred in the robotic manipulator. The cause of the failure had not been completely determined however vibration has been noticed to travel from the spring through the robotic manipulator into the mounting table. The expensive repair of the manipulator has added concerns if vibration could be the cause of failure. For precaution, a solution has been proposed to develop a vibration damper to absorb excess energy from the spring. The damper is design from rubber sponge material which is placed as a cushion for the accelerated slider-cam. In Figure 2.9, the vibration damper is illustrated with slider-cam

locked into the trigger mechanism with the helical spring compressed. Now when the trigger is disengaged the spring is released and the slider-cam begins to accelerate to open the grippers. In Figure 2.10, the slider-cam makes contact with the vibration damper before the end of allowable motion path. With this design the vibration from the sudden stop of the slider-cam is reduced and absorbed partially by the damper. The critical part of this type of damper design is the correct installation in the traveling path of slider-cam. In case of incorrect installation the gripper opening can become partially restricted. The correct gripper opening should be checked when components are removed or replaced.

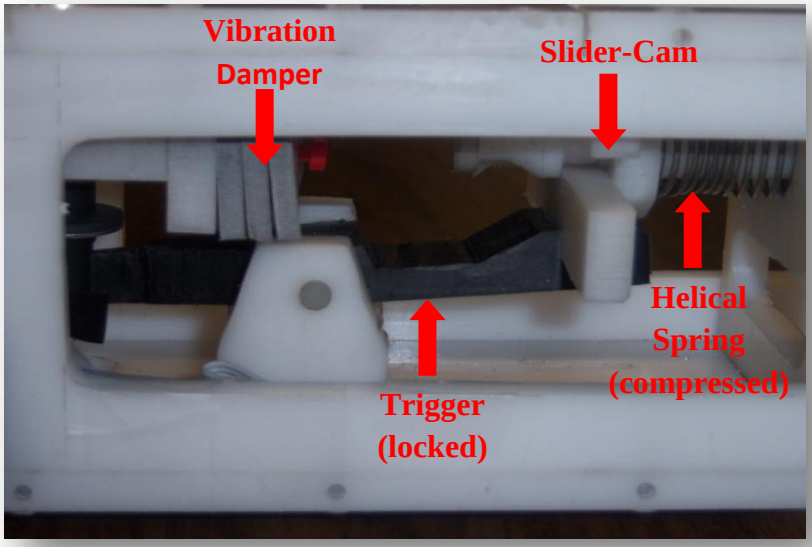

Figure 2.9: Vibration damper before the trigger mechanism is released.

(No contact between vibration damper and slider-cam)

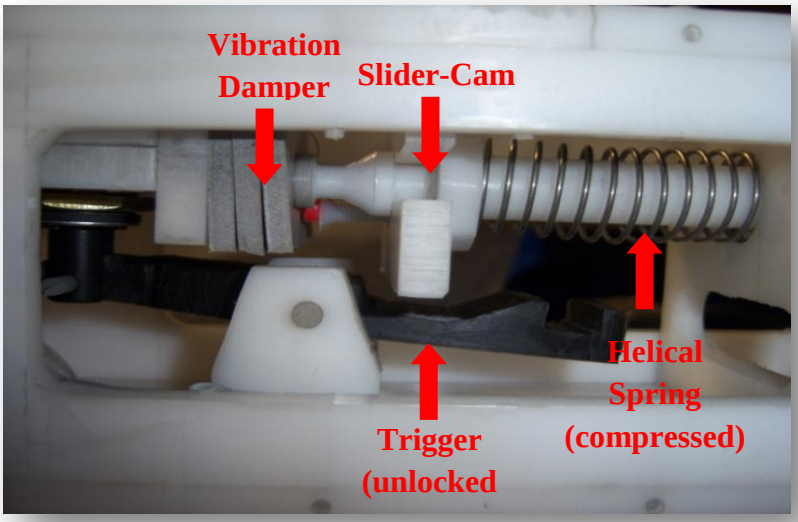

Figure 2.10: Vibration damper after the trigger mechanism is released.

(Full contact between the vibration damper and slider-cam)

CHAPTER 3 – Structural Analysis

3.1 Introduction

Structure analysis has been performed to establish high stresses and deformation areas found in the end-effector prototype. In this analysis a predetermined clinical experience force of 24.5 N (5.5 lbs.) will simulate an operational loading environment. The stress and deformation analysis is carried out using simulation software. The cantilever support which this prototype represents is expected to have minor deflection. The safety factor and error results from this analysis will be discussed at the end of this chapter. The conclusion of this analysis is summarized in Table 3.1.

3.2 Displacement Analysis

In Figure 3.1 the illustration shows a mesh analysis with gradual representation of structure displacement in a cantilever support configuration. The result from the software analysis has concluded a maximum displacement of 0.45 mm (0.018 in) has occurred on the non-supported end of the structure. The needle vertical displacement has also been determined using a point node option from the software to be at 0.38mm (0.015 in). This calculation only shows the deflection of the end-effector under the needle resistance.

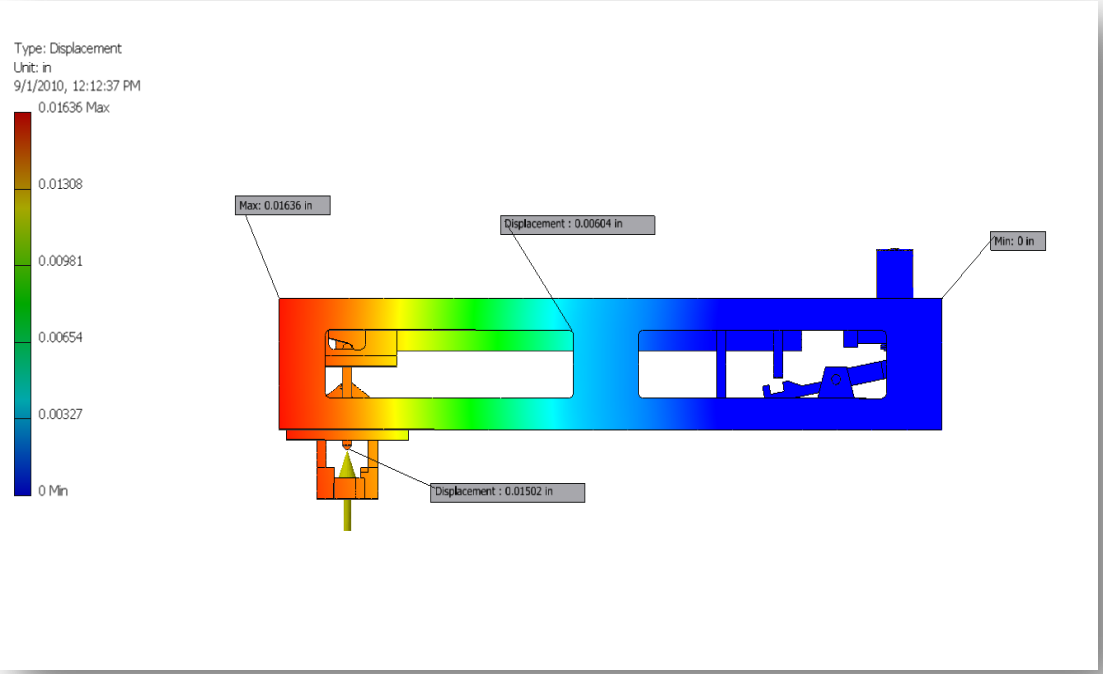

Figure 3. 1: Prototype deflection analysis using simulation software.

3.3 Stress Analysis

In the stress analysis the maximum principle stresses had occurs on the centering rod component which supports the needle direct insertion force. The mesh representing this analysis is illustrated in Figure 3.2 with observed maximum stress of 14.87 MPa (2.16 ksi). The remaining components and structure experience lower magnitudes of stresses which initially were not visible. For proper illustration the range in the mesh scale had been adjusted to maximum stress of 827.4 kPa (0.12 ksi) using trial and error. With this adjustment, visibility of small stresses had been revealed in structural around fillets. The yield strength of Acetal Copolymer material is noted to be at 68.26 MPa (9.90 ksi) which is point at which material will deform plastically. In result, it has been determined that there will be no permanent deformation under the force of 24.5 N (5.5 lbs.) applied to the needle. The maximum stress located on the centering rod is still below yield strength of Acetal Copolymer (2.16 < 9.9 ksi). The end-effector structure stresses determined from the fillets (fillets range: 0.11 – 0.08 ksi) are significantly lower than the yield strength (9.9 ksi). With

this evidence the structure under operation force experiences only negligible stress concentrations.

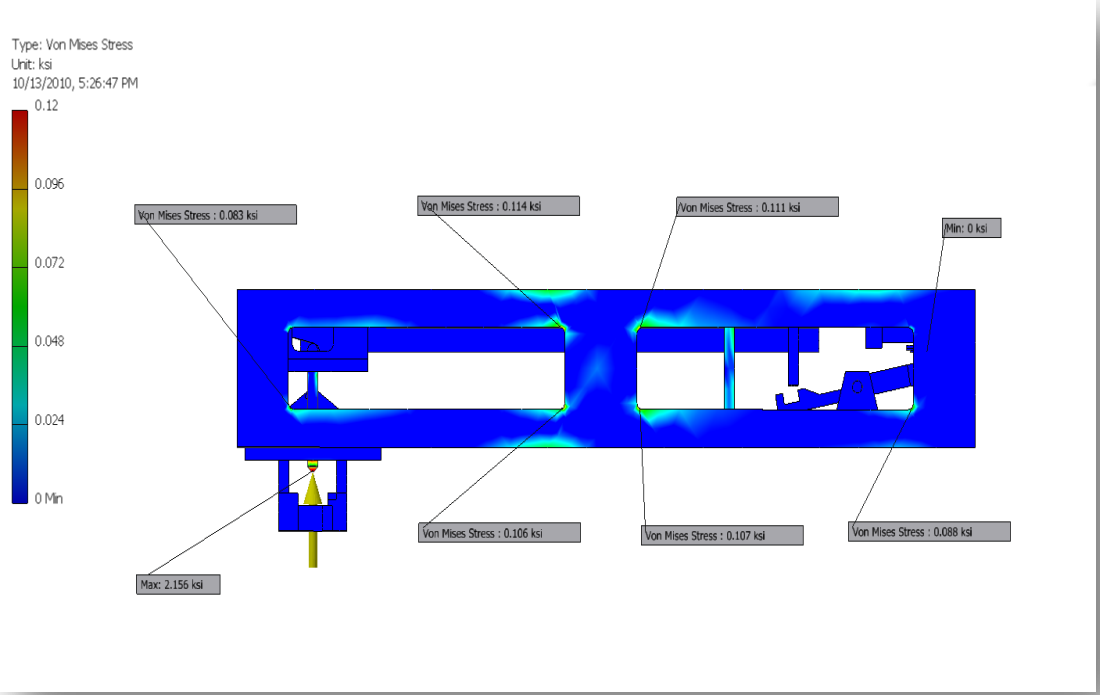

Figure 3.2: Von Mises stress analysis.

3.4 Safety Factor

The safety factor will be determined using the ultimate stress of Acetal Copolymer which is 67.57 MPa (9.80 ksi) and allowable stresses from software simulation. The two allowable stresses which will be used are the maximum stress of the centering rod which is 14.87 MPa (2.16 ksi) and maximum structural stress which is 758.40 kPa (0.11ksi). The safety factors for both stresses will be calculated using Equation 3.1.

$$Safety\ Factor = \frac{ultimate\ stress}{allowable\ stress} \qquad \text{Eq. (3.1)}$$

The safety factor for the centering rod is calculated to be at 4.5 to 1 ratio. Similarly, the calculated safety factor for structure is at 89 to 1 ratio. In conclusion, the prototypes overall safety factor will be the lower value between the two calculated result. Therefore, the prototype safety factor is considered to be at 4.5 to 1 ratio at operation force of 24.5 N (5.5 lbs.).

3.5 Targeting Error

The targeting error is determined using temporary deformation value of 0.38 mm (0.015 in.) from the needle location in respect to the length of the end-effector. The calculated analysis has determined less than 0.01 degrees angle flexing during force of 24.5N (5.5 lbs.) applied at the needle location. The small angle result is due to the end-effector length being much longer than deformation value. Finally, in conclusion the error propagation during procedure is very small and will not have sufficient effect of needle targeting. In a complete system which includes a robotic manipulator, deflection can be compensated using robotic control program.

Prototype Structure Analysis of Needle Force at 24.5N (5.5lbs.)		
	Centering Rod (needle location)	**Structure**
Displacement	0.38 mm (0.015 in)	0.45 mm (0.018 in)
Stress	14.87 MPa (2.16 ksi)	827.4 kPa (0.12 ksi)
Safety Factor	**4.5**	89

Table 3.1: Prototype structure analysis summary.

CHAPTER 4 – Force Sensors

4.1 Introduction

The prototype has been designed to accommodate force sensors in receiving force feedback during biopsy procedure. This additional improvement has shown to be a necessity in providing safety and improved needle tracking during biopsy procedure. Small tissue strains from needle insertion can also be monitored which can cause unnecessary discomfort to the patient. In this chapter a variety of force sensors will be analyzed in approaching all constraints placed on this design. The complete feedback and electronics involved with the sensors will be discussed in Chapter 5.

4.2 Force Sensors Constraints and Proposed Types

The requirement of force sensors for this prototype had been placed on service life, dependability, electrical noise, size, force response, and CT scanning interference. In this design three types of sensors were considered for the optimum solution. The sensors will be individually analyzed with pros and cons to each design.

1. Load Cell - Strain gage type (Figure 4.1)

   This type of sensors measures force by using a foil type strain gage internally attached to a small beam mechanically arranged for specific sensitivity.

   Pros
   - Excellent accuracy and service life.
   - Solid casing for electronic components.
   - Wide range in force feedback.

   Cons
   - Large bulky size even in miniature types in comparing to other sensors of choice.

- The sensor design uses metallic components which will interfere with CT scanning image.
- These types of sensors are more complex in design and are more expensive.

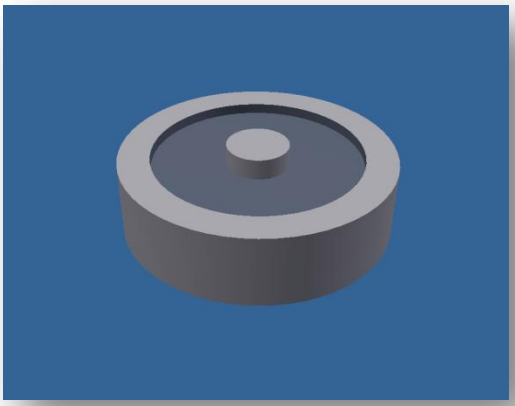

Figure 4.1: Load cell sensor design (strain gage type).

2. Strain Gage - foil type (Figure 4.2)

This type of sensor uses small metallic foil pattern which is stretched under loading in which the resistance of the sensor changes. The sensor is attached to the object by using specific guidelines to prevent sensor from damage. Only specific adhesive should be used with these sensors.

Pros

- Excellent accuracy
- Variety of designs and specifications
- Relatively not expensive.
- Miniature size.
- Low interference under CT scanner.

Cons

- Difficult to install.
- Very fragile and easily over strained during repeating strain cycling.
- Only designed to be used on metallic components due to specific adhesion requirements.

- Change in temperature can affect sensor feedback.

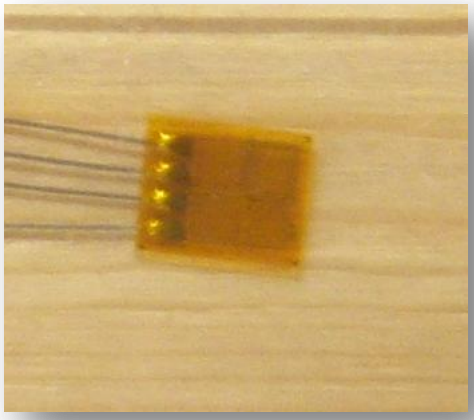

Figure 4.2: Strain gage sensors (foil-type).

3. Force Sensing Resistor – FSR (Figure 4.3)

This type of sensors uses polymer thick film which changes in resistance under loading. With this design the increased in force will result in decrease in resistance feedback. With similar properties to a strain gage this sensor shares no similarities in design.

Pros

- Excellent accuracy and service life.
- Relatively not expensive.
- Stable feedback response under loading.
- Miniature size.
- Low interference under CT scanner.

Cons

- Not design for precision measurements like strain gage.
- Connections can be easily damaged if wires are not constrained properly.
- Change in temperature can affect sensor feedback.

Figure 4.3: Force sensing resistor (FSR).

With the present available solution only two sensors had been determined to satisfy design criteria. The two sensors are the strain gage and the FSR. With priority on low CT scanning interferences from metallic sensors the load cell had been eliminated due to bulk metallic case. In Chapter 6 the CT scanning imaging analysis of prototype will reveal minor imaging interferences of the optimum design.

4.3 Testing of Feedback Response in the FSR and Strain Gage Sensors

In previous section constraint analysis considered only two types of sensors as feasible solution. In this section these two sensors will be tested in feedback response using an oscilloscope to determine stability and response. During feedback testing the FSR sensor had proved to be more stable than a strain gage. The results clearly concluded that a full-bridge strain gage was inferior to FSR sensors. The strain gage response would indicate lower voltage amplitude (micro levels), visual electrical noise, and temperature interference sensitivity. In FSR sensors the response would have wider amplitude range, stable linear response, and limited temperature interferences. Similarly other benefits of FSR sensors included wider flexibility in operation voltage and current settings. Typical strain gage operation current usually carries maximum settings in micro levels which increase difficulties in designing electronic board with single power source. The clear choice in feedback response is the FSR sensors.

4.4 Testing of FSR and Strain Gage Sensors in the Prototype Design

In this section the two feasible solutions will be installed into the prototype for testing sensors in the proposed design. For each sensor the prototype will include minor changes in design to accommodate the function of the sensors. The first sensor which will be tested is the strain gage. The strain gage had been installed on prototype early designed plastic columns made from Acetal Copolymer. The column design would use strain gage in Wheatstone bridge configuration and measure bending in the columns. During testing phase it was found that the strain gage would dislocated after repeated bending cycles and feedback would be lost. Surface treatments had been applied on columns in the locations of the strain gages to increase friction. During retesting of the strain gage it was revealed that surface treatments on Acetal Copolymer will only temporarily increased adhesion. The strain gage once again will dislocate under repeated bending cycles. With the strain gage not being sufficient solution the prototype had been redesigned to adapt the FSR sensors. In the FSR configuration the sensor only measures compression without torsion or bending which was the failure cause of strain gage. The set of four sensors had been adapted to the prototype design to measure horizontal needle forces as illustrated in Figure 4.5. For this configuration only minor adhesion is used to constrain the sensors in the locations. The FSR sensor testing has revealed no failure under repeated pressure forces from installed needle. The final choice for the prototype design is the FSR type sensor.

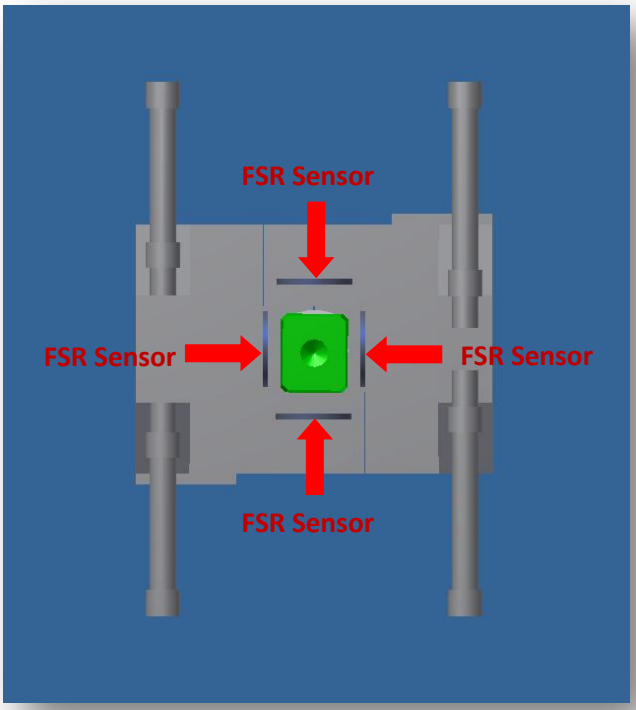

Figure 4.4: The FSR sensor configuration installed in the gripper around the needle.

(Gripper top-view)

4.5 Results

The analysis results concluded that the sensor of choice for this biopsy system is the FSR sensors. The FSR sensors performed better in feedback response and in function with the prototype design. The failure of strain gage had been found in poor adhesion properties to plastics and unsatisfactory sensor response in feedback. There were other complications of the strain gage which included replacement difficulties, fragile design, and reduced lifecycles. The known benefits of the strain are the compact size for less CT interference and higher accuracy. Even that the FSR sensors are not for precision measurement (FSR accuracy 5% - 25%) when comparing to a strain gage (strain gage accuracy 0.10%), the FSR had performed better for this design.

CHAPTER 5 – Control System Function and Design

5.1 Introduction

The control system functions in combination control of robotic manipulator, needle gripper, and sensory feedback system. For the robotic manipulator a special computer system allows program or manual key pad entry for controlling the robot. For the needle gripper a special controller has been designed to control the needle release. The controller includes a main circuit board which is connected with every control device in this system. The main circuit board carries automated safety needle release feature, computer or manual needle release control, and power distribution to other devices. In the sensory feedback the system provide real-time force feedback from the set of FSR sensors mounted on the gripper. The system consists of FSR sensors, data acquisition board (DQA), and a computer station. The sensory feedback is also part of the main circuit board which uses the FSR sensors feedback for controlling the safety needle release feature. The main circuit board for safety is concealed in a remote case which is designed with easy accessible control switches and wiring connectors. For security the control case had been designed with a master power switch key which will prevent unauthorized users from any function.

5.2 Overall Composition of the Control System

The overall composition of the control system is illustrated in Figure 5.1. The major electronic components are defined as follows:

- Remote Controller

The remote controller establishes communication and control with every device in this system. The system is connected in series of cables in the back on the controller.

- Power Supply

The power supply provides electricity required by the solenoid, feedback sensors, and other electronic devices. The preset power settings are at 26 Volts DC and 1.2 Amps.

- Data Acquisition (DQA)

Data acquisition establishes real-time communication between the feedback FSR sensors and computer software. The DQA collects the sensor feedback in real-time.

- Robotic Manipulator Computer

This computer provides robotic manipulator controls and other systems such as output and input functions using software or key pad controls.

- Solenoid

The solenoid provides electrical function in controlling in releasing biopsy needle.

- Feedback Sensors

The feedback sensors provide forces present on the biopsy needle.

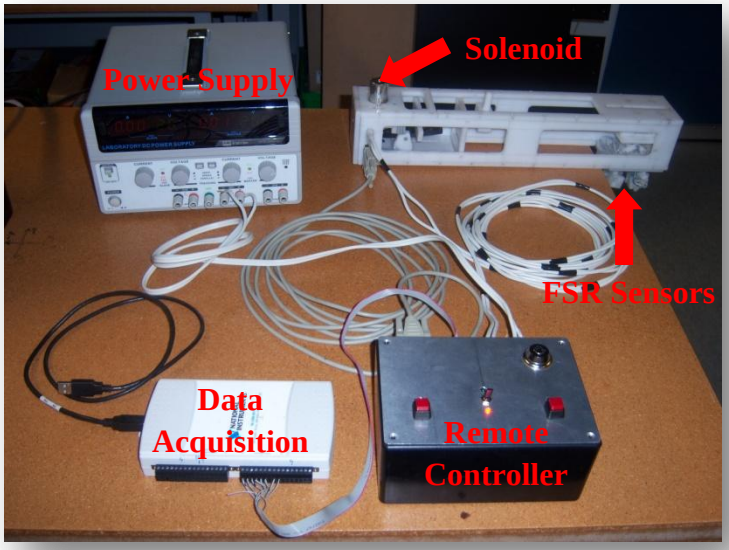

Figure 5.1: Overall composition of the control system.

(Robotic Manipulator computer not shown)

5.3 Circuit Design Introduction

The circuit board has been design from variety of commonly available electronic components such as resistors, transistors, relays, diodes, and operation amplifiers. The purpose of the circuit has been to adapt all the function associated with the end-effector controls except for controlling the robotic manipulator. In this circuit design all the inputs and outputs has been predetermined to account for all electronics requirements. The following list below summarizes all the necessary inputs and outputs which had been adapted to the circuitry. (The numbering of the following list refers to the interlocking connectors which are located on the back of remote controller illustrated in Figure 5.10)

1. Power Source (Input) – The circuit receives and supplies power to other components associated with the end-effector controls which include solenoid, FSR input voltage, diodes, transistor, relay, and operation amplifier. The connection supplies 26 Volts input to the board.

2. Solenoid (output) – The circuit board provides output voltage to the solenoid in case the needle release is commanded. Voltage supplied varies on power source settings.

3. Data Acquisition - DQA (output) – The feedback received from the FSR sensors (input) is transmitted through the circuit board to data acquisition (output) connection. The data acquisition provides real-time feedback using Lab VIEW software program installed on to the computer. Voltage supplied varies on force placed on the FSR sensors.

4. FSR Sensors
   a) (output) – The circuit board provides output voltage which is send to the FSR sensors. The voltage to the sensors is adjustable using variable resistor located on the board for calibrations. Voltage supplied varies on calibration and power source settings.

   b) (input) – The circuit board receives FSR sensor feedback as an input voltage signal which is transferred to the automatic release circuit and the data acquisition output. Voltage supplied varies on force placed on the FSR sensors.

5. Computer Controlled Needle/Trigger Release (input) – This input controls needle release using computer software. The connection supplies 5 Volts input from the computer to the board. The computer receives 5 Volts from secondary power source.

5.4 Main Circuits Designs

The main circuit design consists of combinations of existing predesigned circuits and custom modifications to adapt to all the application of the prototype. The safety needle release feature has been adapted from a predesigned circuitry called threshold switch circuit. In Figure 6.2 the threshold switch circuit illustrates a controlled switch which is triggered using a specific force applied on the FSR sensor. The circuit functions using an operational amplifier (op-amp) which output is an impulse voltage when minimum required voltage is applied on the input side. Since the FSR resistance decrease in respect to the force then the sensor can be used to control voltage on the input side of the op-amp. The variable resistor shown in the circuit is used to adjust input voltage and FSR sensitivity for controlling the op-amp output (impulse voltage). When the op-amp input voltage is satisfied then the output impulse can be used to control devices like a switch. For controlling high power devices a transistor will be required to prevent damage to the op-amp. However, if the controlled device exceeds the operation of the transistor another switch called a relay can be added.

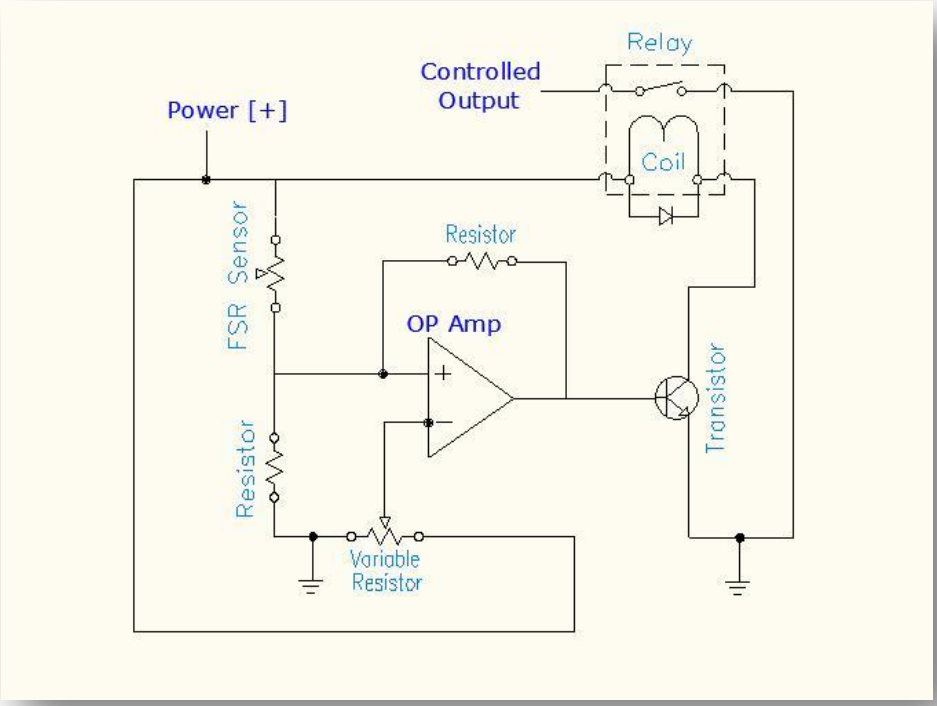

Figure 5.2: Threshold-switch circuit for automated needle release.

For the first main circuit design the threshold-switch circuit (Figure 5.2) is modified to adapt a function from one into four FSR sensors. The first circuit design is illustrated in Figure 5.3 where the threshold circuit is modified with additional FSR sensors. The sensors outputs in Figure 5.3 are separated by addition of diodes used to preserve individual sensor feedback. During testing of this first circuit design the safety needle release feature had worked excellent and had been tested with each FSR sensor for proper function. However, a problem has occurred in this circuit where individual sensor feedback was lost and for each sensor response other sensors generated the same feedback. The investigation of the circuit had concluded that signal separation using diodes are ineffective. The tolerance in diodes allows small current to pass against the direction of diodes resulting in combined feedback in this first circuit design.

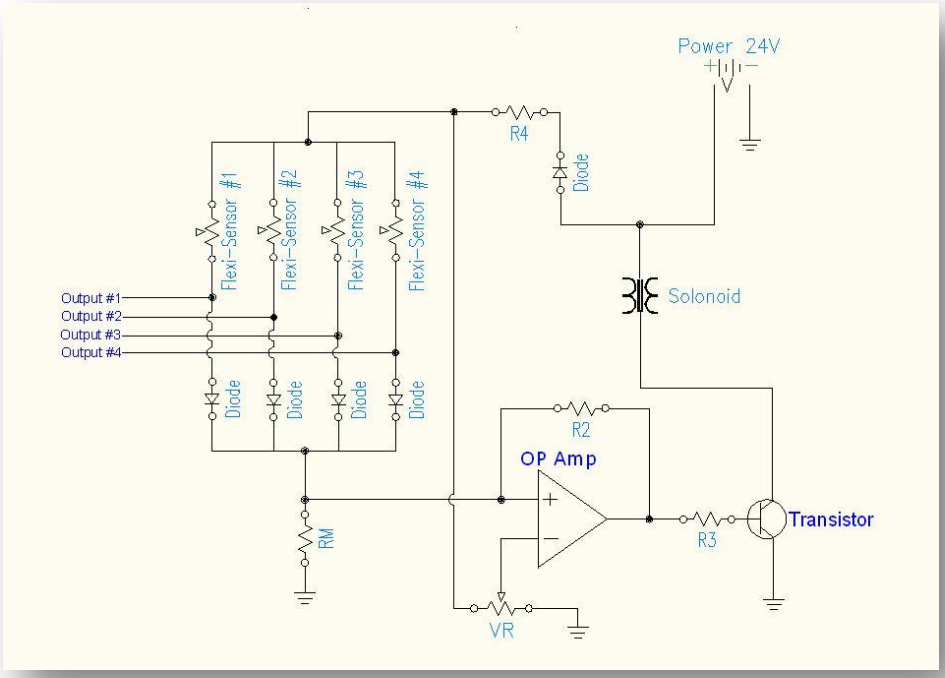

Figure 5.3: The first proposed main circuit diagram with automated needle release.

In the second main circuit design the FSR sensor individual feedback was restored. The solution to the individual feedback loss had been the introduction of individual op-amp for each FSR sensor. In Figure 5.4 the second and final circuit diagram illustrates corrected automatic needle release circuitry with detail components and controls. The basic function of the threshold switch circuit (Figure 5.2) is still the same with only changes in addition of extra op-amps. In real op-amps chip additional power source is required and it is shown in the final circuit diagram. The trigger release for this circuit is controlled by four separate components which include two relays and two simple momentary switches that individually control voltage to the solenoid. The outputs from the op-amps are connected to a single transistor which controls the first relay. The transistor output voltage is controlled by a switch which allows deactivation of the automated safety needle release circuit. The second relay in this circuit is controlled by the robotic manipulator computer output voltage. This allows a trigger release to be controlled using a computer program. With the use of electromagnetic components such as solenoid and relays electrical noise had been found to occur on the sensor feedback screen during these components operation. The solution had been to adapt diodes across these electromagnetic components to reduce high voltage spikes which can damage other electronics. In the FSR sensors circuitry additional variable resistor has been adopted on the top of this circuit to control input sensor voltage. For the

sensitivity control of op-amps output using FSR sensors a single variable resistor is added in the bottom of the final circuit similarly shown in the threshold switch circuit (Figure 5.2). For the data acquisition board the FSR sensor voltage is measured between the sensor output and circuit ground.

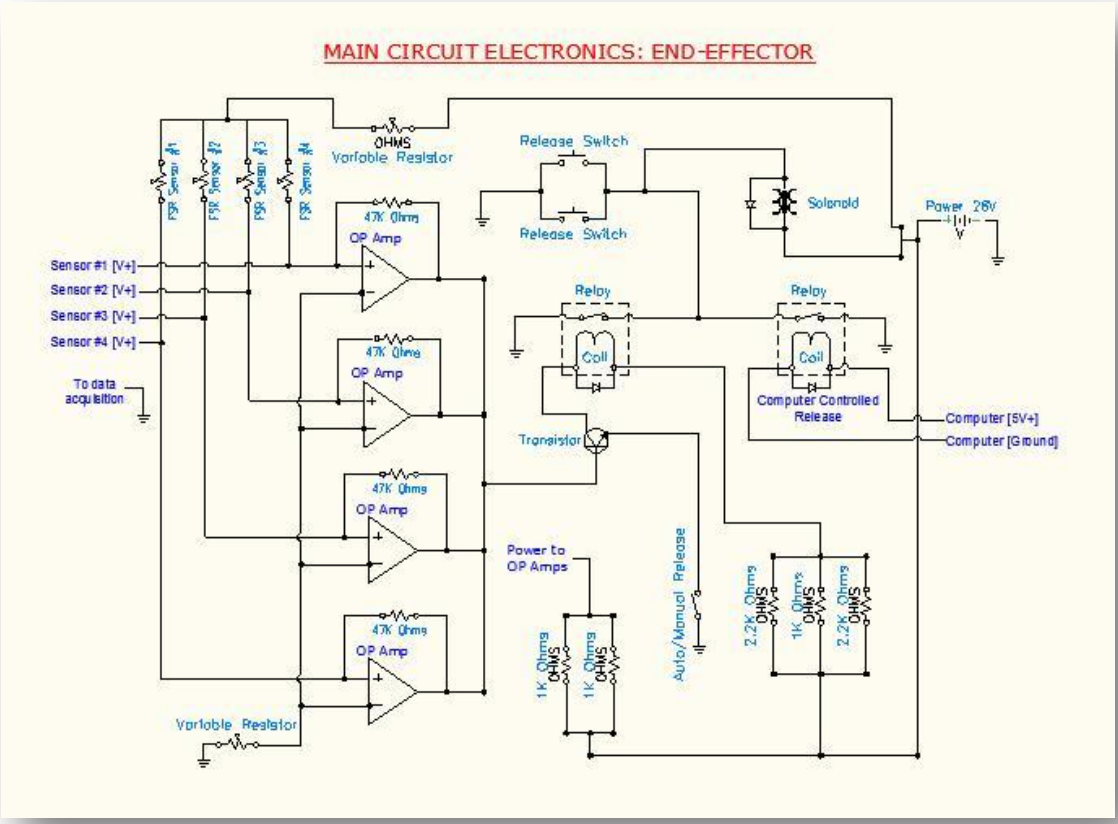

Figure 5.4: The second proposed main circuit diagram and the final solution.

The voltage in the final main circuit is increased from 24V to 26V difference from the first circuit design. The circuit can operate in the ranges of 25V to 28V without damage. It should be noted that changes in circuit operational voltage will require sensors recalibration. If the voltage would be set to the maximum of 28V the sensor sensitivity will increase and the sensors would reach maximum amplitude with less force applied. The Figure 5.5 illustrates completed final design circuit with components layout. In this final circuit some critical electronic components such as transistor and operational amplifier had been designed to be easily replaced. These sensitive components are held in place by retention clips which

are soldered to the circuit board. Similarly the external wiring connected to the circuit board is designed to be easily disconnected using special terminal connectors. In conclusion, this circuit board has been designed to provide reliable control of all the features. Independent circuitry for solenoid is designed to provide multiple release control in case of failure. The automatic needle release feature provides final safety precaution to prevent injury to the patient under abnormal needle forces.

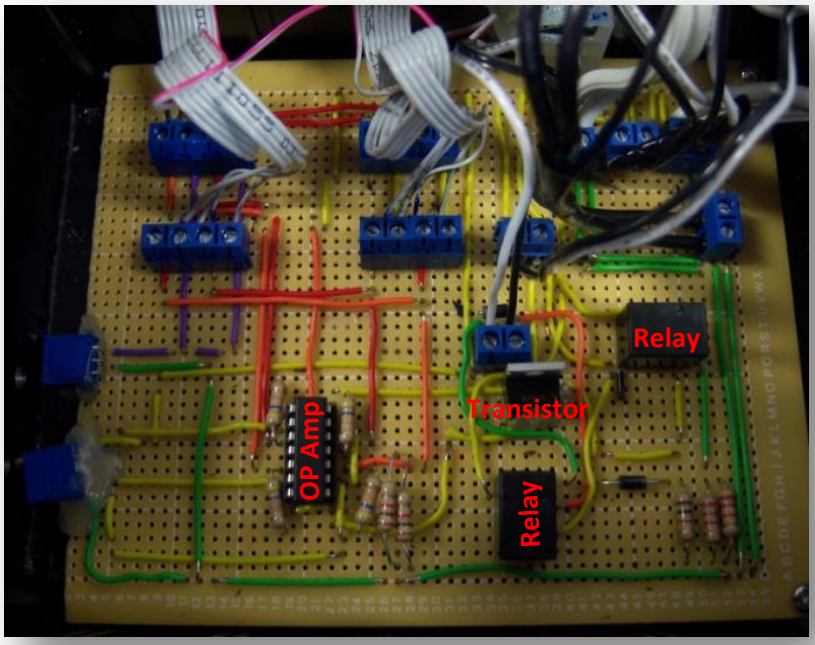

Figure 5.5: The final circuit design.

5.5 Sensor Calibration

The sensor calibration is performed using mechanical and electrical adjustment. The first adjustment is performed using electronic settings in the end-effector controller. In Figure 5.6 the illustration shows two adjustable resistors which are used for calibrating sensors voltage and adjusting sensitivity of the automatic safety needle release feature.

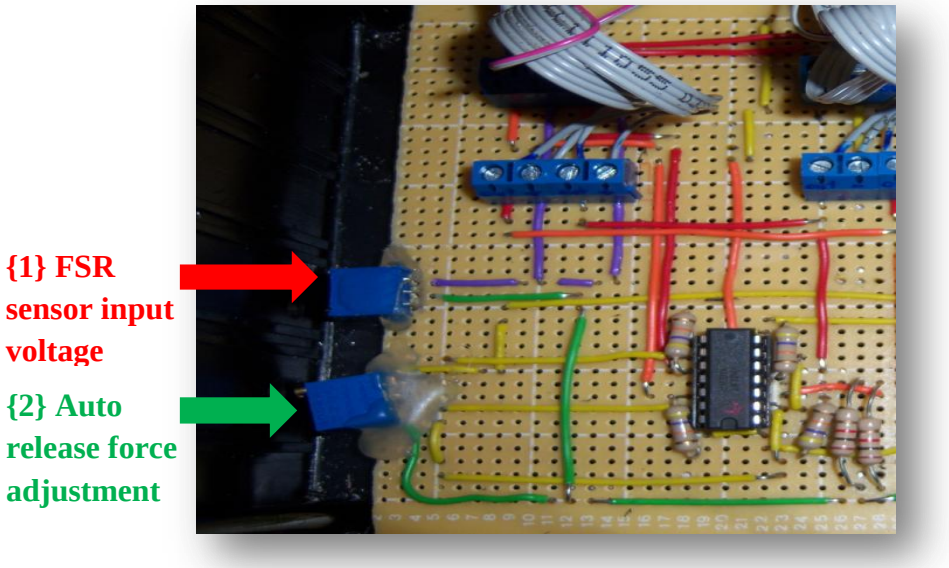

Figure 5.6: The electrical adjustments on the circuit board for the FSR sensors and automatic needle release.

The FSR sensor input voltage is the first adjustment made to calibrate the system. For the first calibration a separate set of FSR sensors are used as shown in Figure 5.7. The sensor force response adjustment is performed under real-time feedback. Similarly, at the same time the auto needle release feature function should be confirmed. In case when the FSR sensor input voltage is adjusted too low the automatic safety needle release feature can delay or not function. Therefore, both adjustments should be carried out to determine the optimum setting required. The adjustment is simply performed from the outside of the control case using two small openings which are aligned with the variable resistors. The adjustment requires a small flat screwdriver which is inserted through the side of the case.

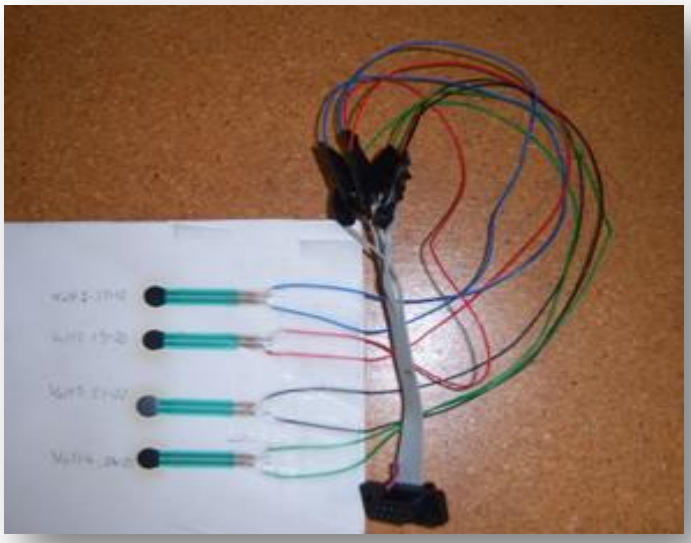

Figure 5.7: Set of external FSR sensors for calibration.

The last adjustment is performed using mechanical screws located on the gripper. The calibration set of FSR sensors are disconnected and the FSR needle sensors located in the gripper are connected for calibration. The mechanical screws located on the gripper illustrated in Figure 5.8 allow the distance between the sensors and the needle to be adjusted. With this adjustment the sensors sensitivity and needle grip adjusted for optimum settings. The adjustment is performed under real-time feedback with needle installed. The sensitivity and gripper tolerance is checked by flexing the needle in horizontal directions. The automated needle release is also checked at this stage to determine proper function. After finishing mechanical calibration another grip adjustment may still be required during needle targeting testing in Chapter 7.

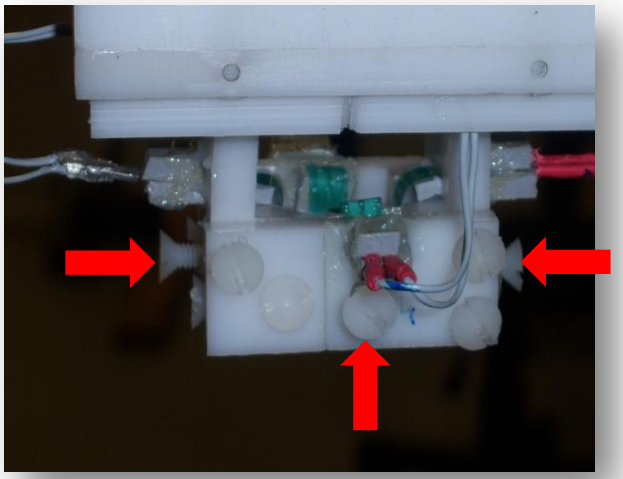

Figure 5.8: Mechanical FSR sensors screw adjustments on the gripper.

(Only three adjustment screws are visible out of four on this illustration)

5.6 Controller Case Design

The control case is designed to secure electronic components such as the circuit board, control switches, and wiring connections. The circuit board is concealed inside the control case with capability of easily disconnecting from any wiring connections as shown in Figure 5.5. The top panel of the case is designed with control switches as shown in Figure 5.9. In the top panel there are three types of switches with LED indicators to illuminate the switching function. The first type of switch is the lock key power switch which is the main power control for the circuit board. When power is switched ON one of the LED indicators around the automatic release selective switch will illuminate. The next type of switch is the automatic release selective switch. This type of switch controls automatic safety needle release function. During needle loading procedure this switch is required to be turned OFF to prevent premature needle release. In other situations this automatic release function should be always set ON as a safety precaution. The last type of switch is the manual needle release switch. This type of switch is a momentary type which requires only a single touch to release the needle. Due to importance of this manual needle release two switches are installed on the top panel of the case.

Figure 5.9: Control case top switching panel.

The back of the control case had been designed with interlocking connectors as illustrated in Figure 5.10. There are a total of five different connectors which from the inside of the case are connected to the circuit board. The difference in connectors prevents the user from crossing wires which can damage the circuitry. In Section 5.3 description and function of the individual connector are summarized in detail.

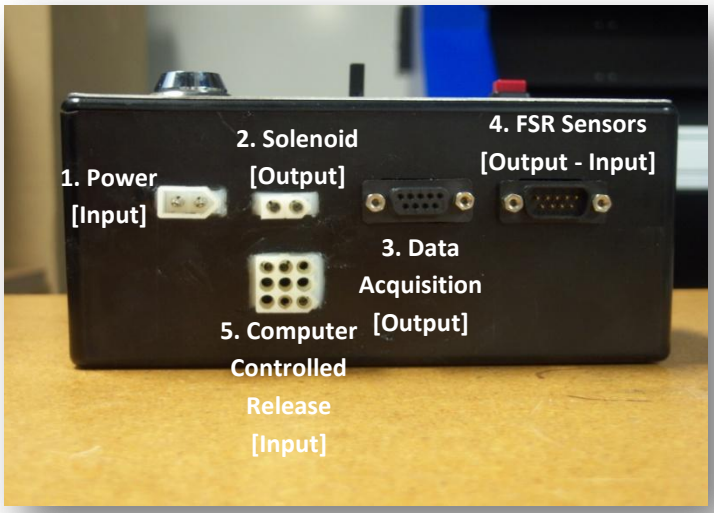

Figure 5.10: Control case input-output rear connectors view.

5.7 Needle Release Controls

The needle release control is the most critical part of biopsy procedure. In case of emergency or during normal operation the needle control is important. Due to the importance placed on this control feature there are three electrical needle releases designed into the control system. In the following paragraphs below individual needle release will be described in detail.

The first release is controlled using one set of manual momentary switches located on the top panel of the control case as illustrated in Figure 5.11. For convenience to the user the location of these switches are placed in two opposite corners. The user may choose the closest switch when instant release is required. For safety reasons these two momentary switches are connected to the circuit board using independent wiring in the simplest circuitry without transistor or relays. During experimental testing one of the momentary switches had failed to release the needle. Immediately the second backup switch was used and needle was released. The cause of failure was determined to be a broken wire caused by frequent removal of the controller's top panel during early design improvement stages. This shows how safety features may prevent delays or a total failure.

The second type of needle release is controlled using a computer output voltage signal. This computer output can be controlled using any modern computer programing software like in this case we used C++ compiler. In this control system the robotic manipulator computer supplies the output voltage which is applied to the relay that controls the solenoid.

The last type of needle release is automatically controlled by the automated safety needle release feature. This system is the most sophisticated in this electronic design when comparing to the other two release control methods. This release function works by constantly monitoring force feedback from the FSR sensors. This safety feature can be engaged using a toggle switch during procedure and require to be disengaged during needle reloading. This needle release system function is fully automated when FSR sensors determine higher than normal force imbalance. In result the system releases the needle automatically to prevent any internal injury to the patient. This safety feature can avoid injuries such as unpredictable motion due to large body movements or large caught.

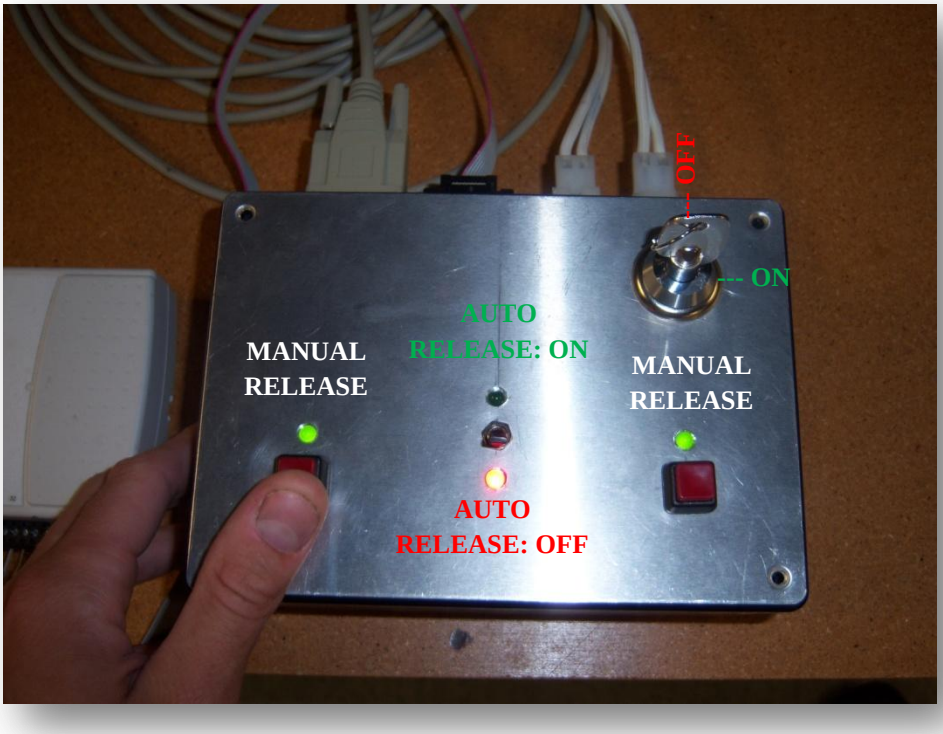

Figure 5.11: The controller top panel view representing manual needle release action.

5.8 Feedback system

The feedback system provides real-time force feedback from the set of FSR sensors mounted on the gripper. The system consists of a data acquisition board (DQA) which is connected to the remote controller using a cable as illustrated by Figure 5.12. Similarly the data acquisition (DQA) is attached to a computer station with Lab VIEW software installed. The Lab VIEW software's front panel is designed to receive the feedback using a graphical representation (waveform graph) similar to oscilloscope patterns. The FSR force sensors changes are received on the positive Y-axis in units of voltage. The voltage increases proportionally to the force which is applied on the sensors. On the X-axis the time frame is measured over maximum cycle of one second. With this graphical representation there is excellent sensors feedback received under any sudden force changes. In Figure 5.13 a simulation shows application of force on the needle at the corner between two sensors. The feedback indicates both sensors responding to the corner force while the opposite two sensors shows only limited response. Then it can be concluded that the current feedback system with all the electronic has performed excellent in terms electrical noise and securing individual sensory feedback.

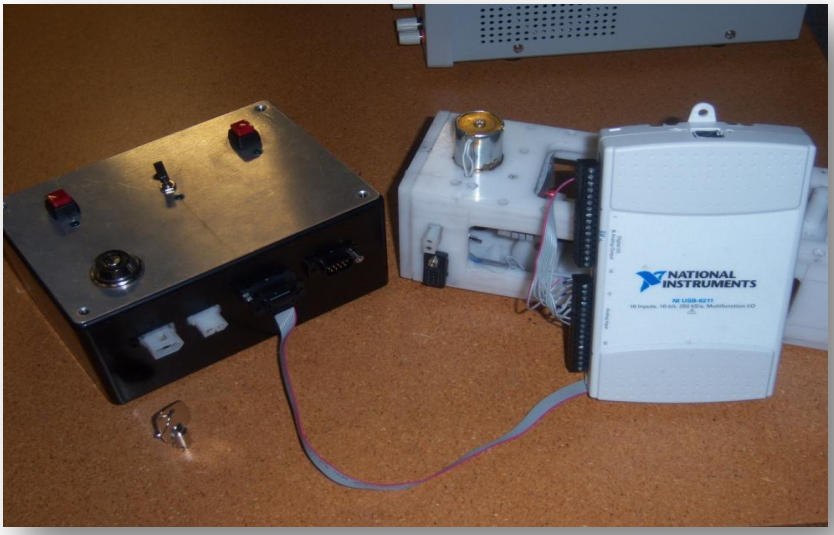

Figure 5.12: Remote controller with data acquisition board.

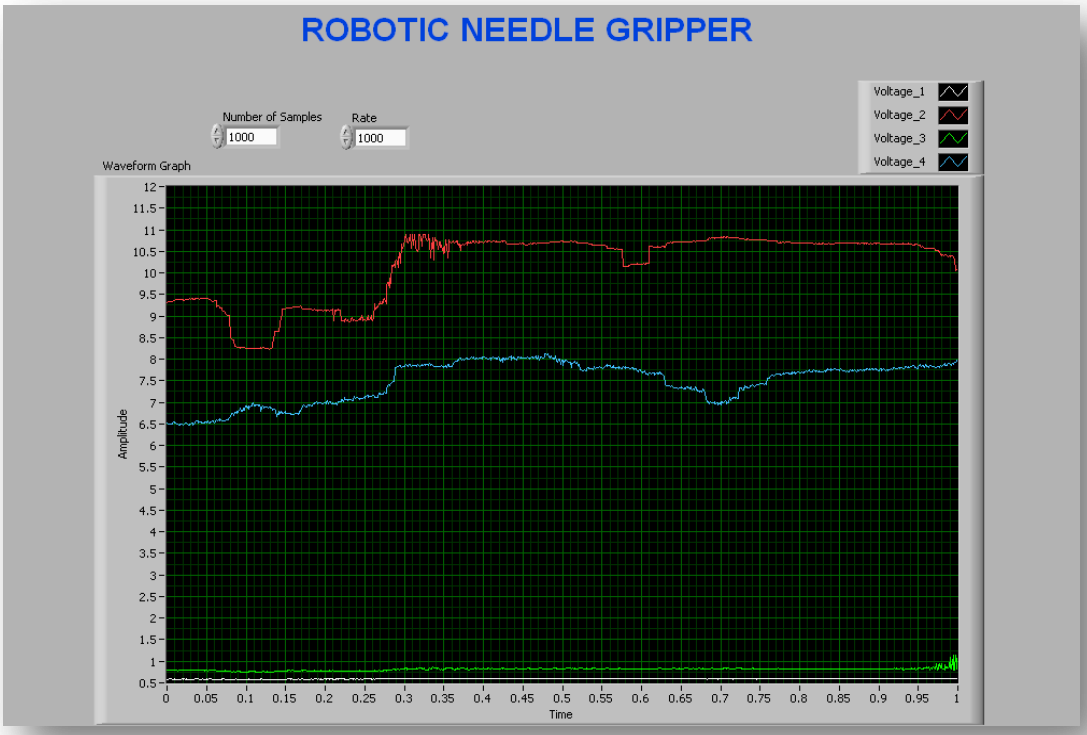

Figure 5.13: Lab VIEW sensor feedback graph.

(The following illustration shows two FSR sensors out of four under corner needle loading condition during response testing)

CHAPTER 6 – Medical Imaging Scanning

6.1 Introduction

In this chapter, the prototype was tested for imaging interferences using a Computer Tomography (CT) scanner. The results reveal the image distortion from critical metallic components which had been used in the prototype.

6.2 CT Scan of the Prototype

The medical imaging device such as Computer Tomography (CT) is currently the most popular image guidance method in needle lung biopsies. The requirement to preserve image quality for CT is to avoid metallic components which form bright streaks in the CT images. The objective has been to design the end-effector with minimum components from metallic origin. Due to the fact non-metallic sensors, actuators, or electrical wires are currently available the current design will include interferences. The understanding of CT imaging features like selective-view window has helped in designing the end-effector to have minimum interferences. The design solution has been to minimize interfering components in the location of the needle. With needle being metallic and produces its own image interference any extra metallic components in the same area can make needle tracking difficult. The proposed design has moved the major interference components a specific distance from needle location. The safety distance that has been proposed to be at length of 25.4 cm (10 in) between the needle and the closest major interference component (compression spring). In Figure 6.1 a preview scan has be performed using CT scanner in low resolution mode which illustrates top-view of the end-effector. Now in the top-view the high interfering and low interfering regions are identified and marked on the Figure 6.1. Next, with the selective-view windows feature only the low interference region is selected for more enhanced CT scanning. The high interfering region components are simply excluded from scanning window and have no effect on image quality.

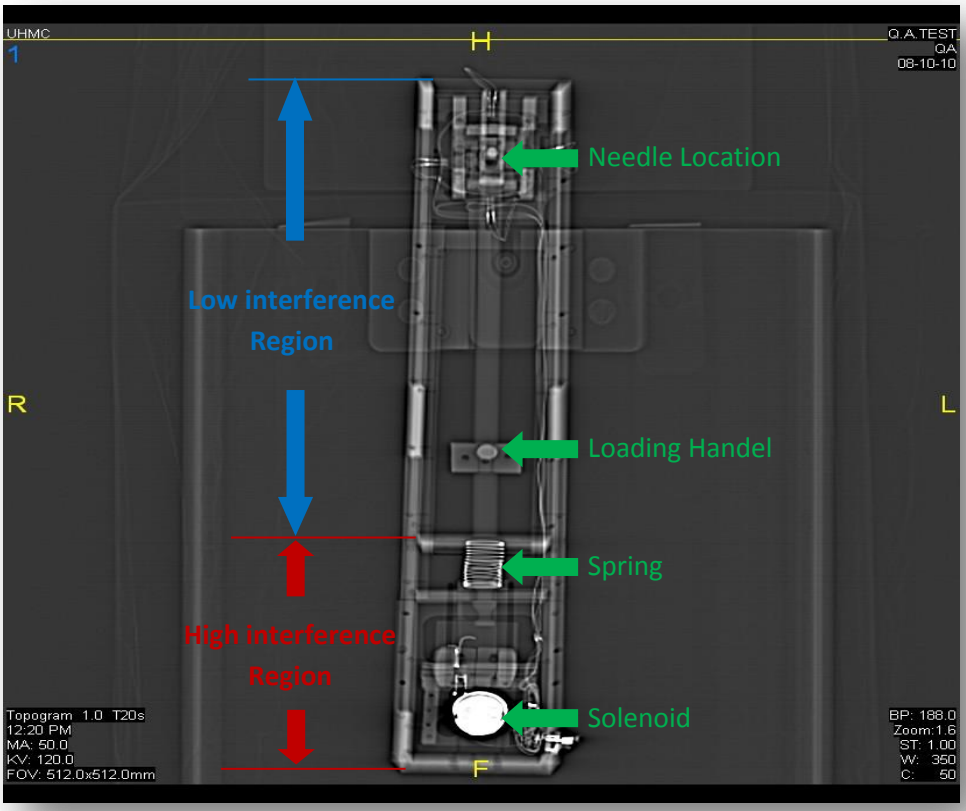

Figure 6.1: CT preview scan of the prototype in the top view.

6.3 CT Interferences

The addition of feedback system to the earlier design had added sensors and wiring in close vicinity of the needle location. Due to this design modification minor image disruptions will now be present in previous designed low interference region. The selection of sensors has been a critical part of this design to keep image interference low. In Chapter 4 the sensor selection had been based on image interference to guarantee a feasible solution. Even that the best feasible solution with the lowest interference was the strain gage (smaller in size) the other factors had eliminated it from optimum choice. The optimum sensor which had been adapted to this design is the FSR (Force Sensing Resistor). In Figure 6.2 the CT scan reveals interferences in vicinity area on the needle. The visible bright streaks represent

interference from the electrical wiring and FSR connectors. It should be noted that FSR sensor itself has almost no interferences as previously it had been expected.

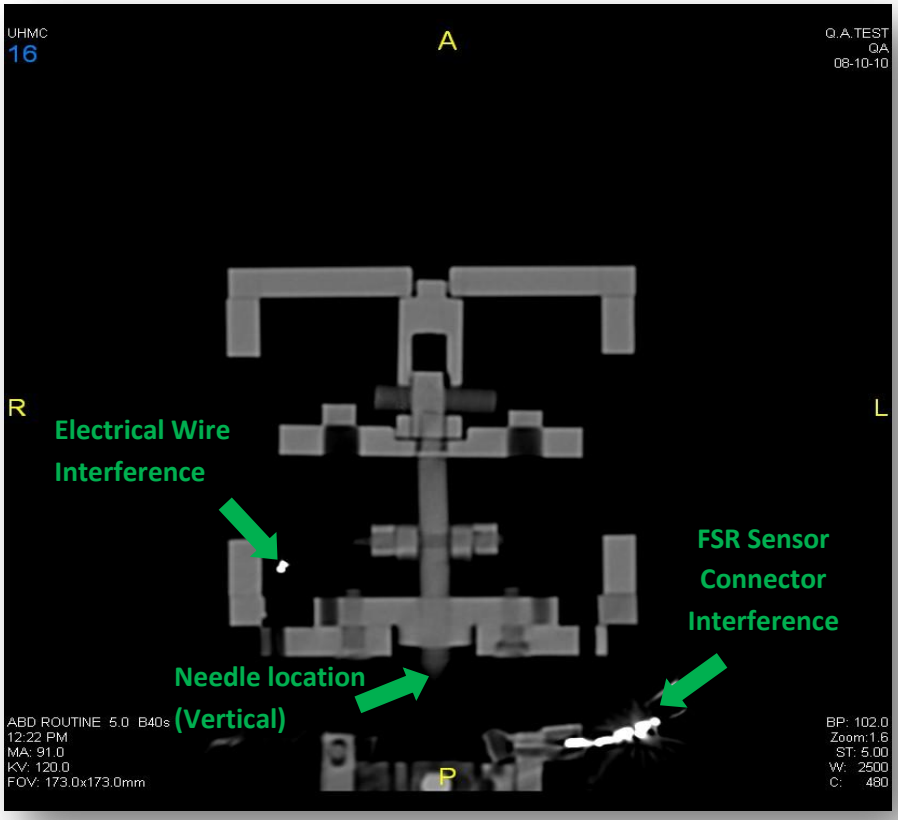

Figure 6.2: CT scanning of the prototype in the vertical cut-view.

(The bright streaks represent metallic interferences in vicinity of the needle location. Needle is not scanned in this illustration)

6.4 Conclusion and Results

In conclusion, the prototype design still maintains good quality image in low interferences region. The zero interference currently cannot be achieved due to the biopsy needle being metallic and interfering with some image quality. However, the interference can be beneficial during needle biopsy. The interfering bright streaks from the needle improve visibility which can help in needle tracking.

CHAPTER 7 – Needle Targeting and Accuracy Testing

7.1 Introduction

In this chapter the prototype will be tested to determine accuracy in placing biopsy needle on target. There will be various testing performed which will include stationary and moving targets. All the targeting testing will be performed using computer software which will control the robotic manipulator. The targets will be a simple soft sponge and a canned pea representing a nodule.

7.2 Needle Target and Automated Safety Release Testing

The first test had involved testing the robotic manipulators repeatability by placing the needle on the marked target which is a soft sponge (Figure 7.1). The use of the soft sponge has prevented any accidental damage to the needle and sensors during the initial testing. The test has been performed numerous times and determined the robotic manipulator repeatability to be excellent on stationary targets. In the second test the robotic manipulator has been tested against a movable target. The target once again was a soft sponge which was propelled around three axes using a motion stage table. Now to coordinate the robotic manipulator and the motion stage table a camera has been used to synchronize these two systems. The camera would use a specific target attached to the motion stage table which would activate the robotic manipulator program. The setup of the motion stage table with the camera is illustrated in Figure 7.2. After the needle was placed on moving target all needle release controls had been tested during this experiment. In result the robotic manipulator and motion stage table has demonstrated excellent repeatability in which needle has always hit the target. The automated safety needle release feature had required minor adjustment and functioned properly in this test.

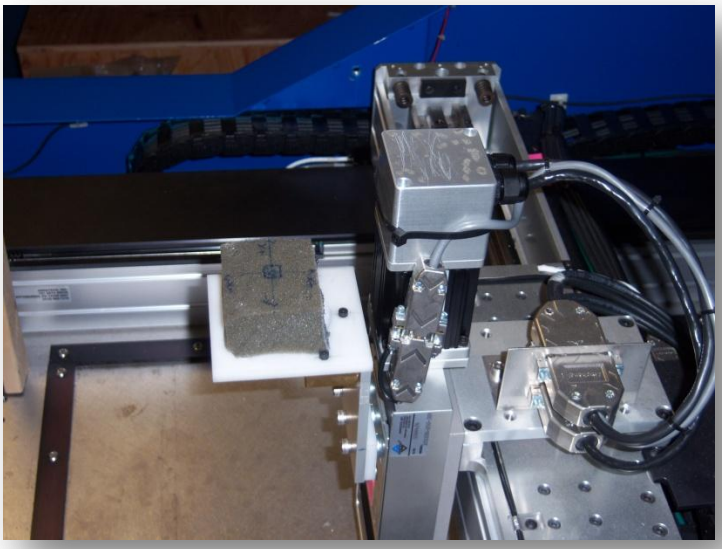

Figure 7.1: Soft sponge test for stationary and movable targets.

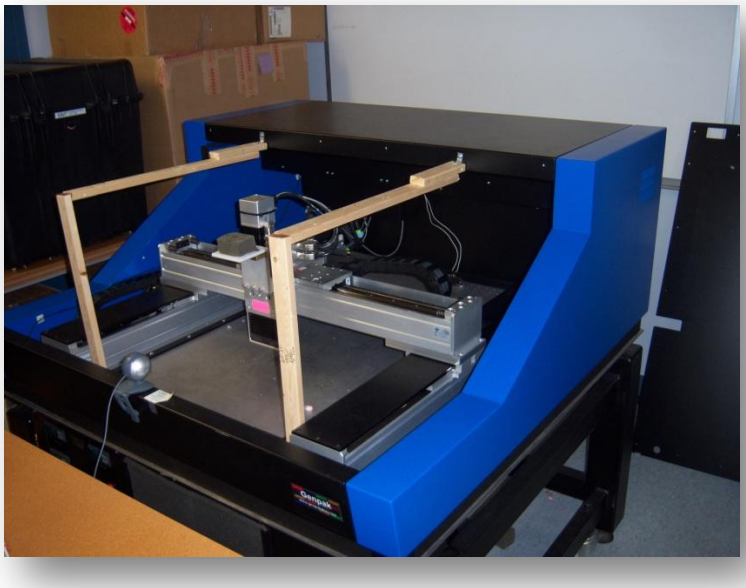

Figure 7.2: Motion stage table with the synchronizing camera.

7.3 Needle Canned Pea and Corn Test

In the third test the sponge was replaced with a plastic container which contains corn seeds and a single pea. The single pea will be a target which will simulate a nodule which would be located in the lung. This testing will indicate the repeatability on the placing the needle in the center of the pea located in the cup. The cup will be placed in motion around three axes using a motion stage table. The robotic manipulator will insert the needle and quickly move up to pick up the pea. In Figure 7.3 the illustration shows a diameter of the experimented pea to be approximately 8 mm (0.315 in). The pea had been marked with a pen in the center to indicate a clear entry point for the needle. In result the needle hit the target multiple times in the center of the pea (Figure 7.4). The pea pickup was not always achieved by the needle due to the pea being too soft. There was some complication in early targeting in the pea test. The problem occurred when the motion stage table had shifted some of the corn seeds and the pea out of positions. The correction has been made to repack the corn seeds and the pea tighter in the cup to prevent additional movement.

Figure 7.3: Recording of the diameter of the canned pea.

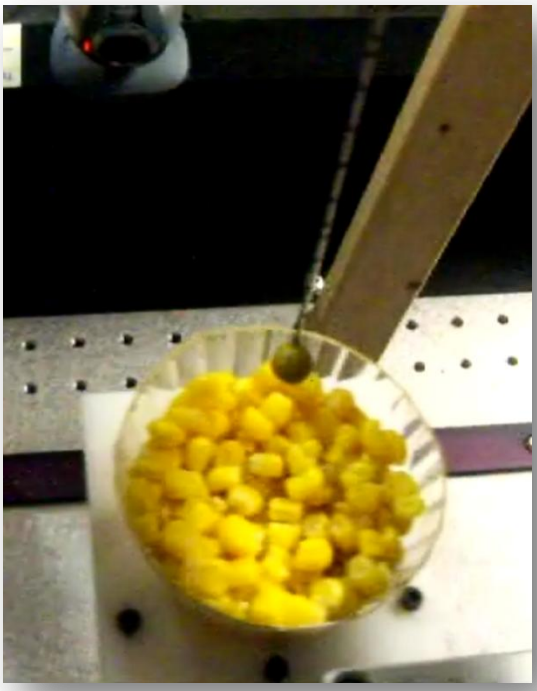

Figure 7.4: Perfectly targeted and picked up pea during movable targeting test.

7.4 Conclusion and Results

In conclusion, the targeting testing had revealed excellent repeatability of the motion stage table and the robotic manipulator which is rated at ± 0.04 mm (0.0016 in) from the manufacturer. The synchronization technique using a camera of these separate systems had also confirmed to be accurate. In the pea test the robotic manipulator had demonstrated placement of the needle in the center of the pea representing a nodule from which the biopsy is collected. The mechanical grippers had also shown excellent needle constrain and stability. The safety needle release feature had also been tested and functioned correctly in releasing the needle.

CHAPTER 8 – Discussion and Conclusion

In this thesis, research had been conducted toward a new technique for lung biopsies. This new system has promising advantages over the manual needle placing technique which the outcome depends on clinician's experience. The proposed solution which had been described is a robotic manipulator that will delivery biopsy needle on target. The proposed system works in a combination of robotic manipulator, robotic needle gripper, and remote controller for the robotic needle gripper.

The detail design included in this thesis provide reasoning imposed on the prototype material, structure design, mechanical design, electronic control systems design, and force feedback. The systems in the prototype had been also tested for structure stresses, mechanical function, electrical systems control, and feedback response. Other testing included image interferences from the prototype using CT scanner and needle targeting accuracy.

In conclusion, this new biopsy system is the next step in replacing the manual needle targeting with a high precision robotic system. The current research helped developed a working prototype designed to carry a standard biopsy needle and place it on the target. The various devices had been adapted to ensure safety for this new biopsy design. The ideal system will provide high accurate biopsy method for every procedure. In the future research the current prototype design will be studied and improved.

CHAPTER 9 – Future Work

The proposed future work on this robotic needle gripper will include improvements in targeting methods. The following topics below will discuss the future research work.

1) Respiratory motion modeling

   The respiratory motion modeling is referring to the modeling of the lungs motion during steady breathing. This study will determine the location of the nodule in relation to the skin surface from which the needle will enter. Due to lung respiratory motion during breathing in relation to almost stationary skin surface the targeting can be difficult. This study will determine the correct motion pattern which will correlate the position of the nodule in relation to the top surface of the skin without breathing interruptions.

2) Needle path planning

   The objective of this study is to determine the correct path of needle entry for reaching the nodule. The nodule is some cases can be difficult in targeting due to interferences from bones and other critical parts in the body. The needle path planning will determine the safest point of entry with least pain for the patients.

3) Needle advancement control

   The needle advance control will use the respiratory motion planning and needle path planning data for targeting the nodule. This system will control the robotic manipulator function and automatically place the needle on target.

References

[1] Kazerooni, Ella A. "High Resolution CT of the Lungs." American Journal of Roentology (2001): 19.

[2] T. Hirose, K. Mori1, S, Machida1, K. Tominaga, K. Yokoi, M. Adachi,. ""Computed tomographic fluoroscopy guided transthoracic needle biopsy for diagnosis of pulmonary nodule"." Japanese Journal of Clinical Oncology (2000): 30(6): 259-262.

[3] D. Shaham. ""Semi-invasive and invasive procedures for the diagnosis and staging of lung cancer I - Percutaneous transthoracic needle biopsy"." Radiology Clinics of North America (2000): 38(3): 525.

[4] Costello, Barbara Wexler & Angela M. "Lung biopsy." www.surgeryencyclopedia.com/La-Pa/Lung-Biopsy.html n.d.

[5] S. K. Carlson, J. P. Felmlee, C. E. Bender, R. L. Ehman, K. L. Cassic, T. L. Hoskin, W. S. Harmsen, H. H. Hu,. ""CT fluoroscopy-guided biopsy of the lung or upper abdomen with a breath-hold monitoring and feedback system: A prospective randomized controlled clinical trial"." Radiology (2005): 237(2): 701-708.

[6] S. K. Carlson, J. P. Felmlee, C. E. Bender, R. L. Ehman, K. L. Classic, H. H. Hu, T. L. Hoskin,. ""Intermitten-mode CT fluoroscopy-guided biopsy of the lung or upper abdomen with breath-hold monitoring and feedback: System development and feasibility"." Radiology (2003): 229(3): 906-912.

[7] S. N. Goldgerg, M. T. Keogan, V. Raptopoulos,. ""Percutaneous CT-guided biopsy: improved confirmation of sampling site and needle positioning using a multistep technique at CT fluoroscopy"." Journal of Computer Assisted Tomography (2000): 24(2): 264-266.

[8] J. de Mey, B. Op de Beeck, M. Meysman, M. Noppen, M. De Maeseneer, M. Vanhoey, W. Vincken, M. Osteaux,. ""Real time CT-fluoroscopy: diagnostic and therapeutic applications"." European Journal of Radiology (2000): 34(1): 32-40.

[9] P. J. Schaefer, F. K. W. Schaefer, M. Heller, T. Jahnke,. ""CT fluoroscopy-guided biopsy of small pulmonary and upper abdominal lesions: Efficacy with a modified breathing

technique"." Journal of Vascular and Interventional Radiology (2007): 18(10): 1241-1248.

[10] S. L. Heck, P. Blom, A. Berstad,. ""Accuracy and complications in computed tomography fluoroscopy guided needle biopsies of lung masses"." European Radiology (2006): 16(6): 1387-1392.

[11] H. K. Bungay, J Berger, Z. C. Trail, F. V. Gleeson. "Pneumothorax post CT- guided lung biopsy." The British Journal of Radiology (1999): 4.

[12] E. K. Paulson, D. H. Sheafor, D. S. Enterline, H. P. McAdams, T. T. Yoshizumi,. ""CT fluoroscopy-guided interventional procedures: techniques and radiation dose to radiologists"." Radiology (2001): 220(1): 161-167.

[13] J. M. Anderson, J. Murchinson, D. Patel,. ""CT - guided lung biopsy: Factors influencing diagnostic yield and complicatuin rate"." Clinical Radiology (2003): 58(10): 791-797.

[14] M. J. Wallace, S. Krishnanurthy, L. D. Broemeling, S. Gupta, K. Ahrar, F. A. Morello, M. E. Hicks,. ""CT - guided percutaneous fine-needle aspiration biopsy of small (<= 1-cm) pulmonary lesions"." Radiology (2002): 225(3): 823-828.